

COVER PAGE

Document downloaded by @DAEL

Fri Nov 27 01:20:04 2026
For personal use

When automatic English translation is provided, only the original document is authentic.
The EAA cannot be held responsible of any translation error

Bibliographical reference

Elimination of Internal Structural Variables through explicit Taylor-Laurent Model Reduction, with Applications to Damped Sandwich Plates, Jean-Marie Lagache and Samir Assaf, Acta Acustica **vol. 98** (Number 2), 2012, pp. 242-262

DOI
https://doi.org/10.3813/AAA.918509

ACTA ACUSTICA UNITED WITH ACUSTICA
Vol. 98 (2012) 242 – 262

DOI 10.3813/AAA.918509

Elimination of Internal Structural Variables through explicit Taylor-Laurent Model Reduction, with Applications to Damped Sandwich Plates

Jean-Marie Lagache[1)], Samir Assaf[2)]

[1)] Architecture Mécanique Moteurs et Transmissions, PSA, Centre de la Garenne, 18, rue des Fauvelles, 92250 La Garenne Colombes, France

[2)] Laboratoire d'Acoustique et Vibration, Ecole Supérieure des Techniques Aéronautiques et de Construction Automobile (ESTACA), 34, rue Victor Hugo, 92300 Levallois Perret, France. samir.assaf@estaca.fr

Summary

This paper introduces and discusses explicit condensation methods based on Taylor-Laurent expansion of dynamic responses. The major contribution is the formulation in free-floating conditions of a "degeneracy theorem", stipulating that Laurent coefficients of an embedded subsystem are always invertible, while those of a free autonomous system are always singular matrices. From this, an original sensitive technique - termed "Covering-Censoring reduction" - where the quality of the results can be checked before condensation is performed, is described and then applied to the problem of vibration and acoustic radiation (transmission loss) of sandwich plates (more precisely, plates with attached constrained layer damping). The method presented in the paper is of great interest in several applications necessitating the condensation of internal and/or secondary degrees of freedom.

PACS no. 43.40. r

1. Introduction

Elimination of internal degrees of freedom and, more generally, reductions in dynamic finite element modeling, far from being reducible to pure algebraic techniques, are difficult physical questions. Indeed, except when it coincides with the initial system to be reduced, an arbitrary part a can never be said to be an autonomous system governed by reduced $\boldsymbol{k}$ and $\boldsymbol{m}$ matrices, but is always subject to internal resonant interactions with the complementary part d should the latter remain unloaded. A given set i of coordinates of interest, say an "interface", will thus rarely constitute an admissible condensation set. The predictable decay of internal interactions when a tends to cover the whole initial system means that the complete reduction problem can be imagined, in its simplest form, as some generalized min-max problem which consists in adjusting the smallest possible a containing the interface i.

To contribute to a better understanding and control of the construction of reduced models in the frequency domain, it is proposed in the present paper to introduce a general class of "explicit coordinate reductions", inspired by experimental practice, which consist in collecting, selecting, and assembling independent receptance observations on the system to be condensed, and then proceeding, if possible, to identify reduced matrices through Taylor-Laurent developments of receptance relations. The general principle of such reductions is described and compared to the more widespread Ritz-Galerkin approach [1, 2, 3, 4, 5, 6, 7, 8, 9, 10] in section 2 of the paper.

An explicit method of reduction of fixed systems is developed in section 3. This results in what can be considered as a block decomposition of Guyan reduction. The advantage, however, is that generalized coordinates can be adjoined to ordinary ones. In addition, the effective control of errors - including the determination of the frequency bandwidth of models - which is known to be a difficult question of Ritz-Galerkin theory [11, 12], can be carried out using the Taylor remainders.

Free-floating systems, despite or maybe thanks to their algebraic complexity, give rise to the formulation of an original "degeneracy theorem", stipulating that Laurent coefficients of embedded subsystems are always invertible, while those of free autonomous systems are always singular matrices. From this, an interesting constructive method of condensation, termed "Covering-Censoring" reduction, also in ordinary or generalized coordinates, can be defined. Following some preliminary conference communications [13, 14, 15, 16, 17], a detailed presentation of the technique is given for the first time in section 4 of the paper. To the authors' knowledge, checking the possibility of reduction to a free-floating subsystem by the spectral inspection of a limited number of matrix coefficients has no equivalent in the Structural Dynamics literature. It should

Received 4 May 2010, Revised 9 May 2011,
accepted 3 December 2011.

© S. Hirzel Verlag · EAA

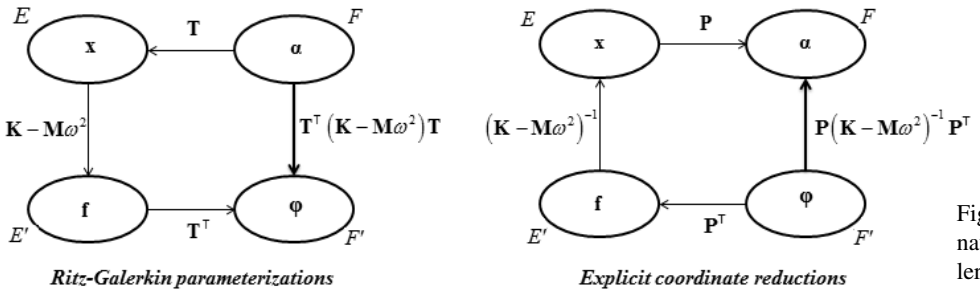

Figure 1. Explicit coordinate reductions vs. Ritz-Galerkin parameterizations.

be noted that the remainders of Laurent series are geometric progressions, which offer the same possibilities as Taylor remainders for the control of errors and the determination of bandwidths. The inherent complexity of the subject necessitates important mathematical complements on Singular Linear Algebra and Pseudo-Inversion techniques. Basic principles can be found in [18] and more specific technical notes in four Appendices labeled A, B, C and D, at the end of the text. Appendix A is devoted to pseudo-inverse solutions to rectangular systems; Appendix B gives the pseudo-inverse solution of square symmetric systems; Appendix C is dedicated to the precise calculation of Laurent coefficients using the preceding general techniques. Finally, Appendix D gives modal expressions of coefficients - based on ordinary or "accelerated" [19] mode-superposition formulae - which are of great help in the analysis of singular systems.

Among various technical fields, the application of the method to modeling of sandwich structures was thought to be a challenging project: first, for the intrinsic interest of the domain; second, for the confrontation of subtle formulations leading to particularly ill-conditioned matrices; and third, for the absolute necessity of completing the basic method to take real damping into consideration. Within the wide domain of modeling of damped structures, section 5 details the reduction of the generic family of 7-dof sandwich models of [20] and [21]. The explicit methods of the above sections are first applied to the reduction of only the elastic part, then real damping is reintroduced on reduced skeletons using the Modal Strain Energy approach [22, 23]. Section 6 concludes the series of examples by revisiting the published experimental results of [24] concerning mean square velocities, and of [25] concerning the Transmission Loss characteristics of viscoelastically damped sandwich plates.

2. Theoretical framework

2.1. General presentation

In Elementary Geometry, using a polar parameterization -$x = r\cos\theta$, $y = r\sin\theta$- is one thing; but adapting the parameterization to the study of a given problem is another thing which demands that the inverse transformation, $(x, y) \rightarrow (r, \theta)$ - known in Mathematics as the "system of coordinates" associated to the parameterization [26] - to be fully mastered. To face well-known difficulties to formulate correct reduction procedures of discrete finite element models in the frequency domain, and to get a better understanding of Ritz-Galerkin parameterizations, $\boldsymbol{x} = \boldsymbol{T}\boldsymbol{a}$, which are commonly used in effective structural reductions, the authors have been led to introduce "Explicit Coordinate Reductions" starting with the definition, $\boldsymbol{a} = \boldsymbol{P}\boldsymbol{x}$, of reduced generalized coordinates in terms of structural ones.

Nevertheless, the question is a little more complicated in Structural Mechanics than in Elementary Geometry: first, because transformations are governed by non-invertible rectangular matrices; second, because transformations concern dual pairs of vector spaces and "natural" duality products associated with the measure of energy. The two types of transformation are outlined in the commutative diagrams of Figure 1. The Achilles' heel is in the choice of relations of the form $\boldsymbol{\psi} = \boldsymbol{T}^T\boldsymbol{f}$ or $\boldsymbol{f} = \boldsymbol{P}^T\boldsymbol{\psi}$ between spaces E' and F' of structural and reduced forces. For the real coordinates and standard duality products that are usually considered, it can *rapidly* be said that the transposed matrices, $\boldsymbol{T}^T$ and $\boldsymbol{P}^T$, represent adjoint operators that guarantee the energetic consistency of approximations, $\langle \boldsymbol{f}|\boldsymbol{x}\rangle_{E',E} = \langle \boldsymbol{\psi}|\boldsymbol{a}\rangle_{F',F}$.

From this, basic equations of motion $(\boldsymbol{K} - \boldsymbol{M}\omega^2) = \boldsymbol{f}$ in the frequency domain, where $\boldsymbol{K}$ and $\boldsymbol{M}$ are the initial stiffness and mass matrices, respectively, and ω is the circular frequency, are readily changed, in the Ritz-Galerkin context, into ready-to-use reduced equations of the form

$$\boldsymbol{T}^T\left(\boldsymbol{K} - \boldsymbol{M}\omega^2\right)\boldsymbol{T}\boldsymbol{a} = \boldsymbol{\psi}. \tag{1}$$

Although such expressions never need to be assembled, it is convenient to say that explicit methods "lead" to equations of the form

$$\left[\boldsymbol{P}\left(\boldsymbol{K} - \omega^2\boldsymbol{M}\right)^{-1}\boldsymbol{P}^T\right]^{-1}\boldsymbol{a} = \boldsymbol{\psi}. \tag{2}$$

The essential of the work remains evidently to derive explicit expressions of this equation using, for example, block-inversion formulae, modal development techniques [13, 14] or Taylor expansion as in the present paper. Reduced coordinates in this context cannot be interpreted as position parameters, as in the Ritz-Galerkin approach. They rather refer to formal combinations of elementary responses to be used in some sort of experimental tests and to proceed, if possible, to the identification of a standard

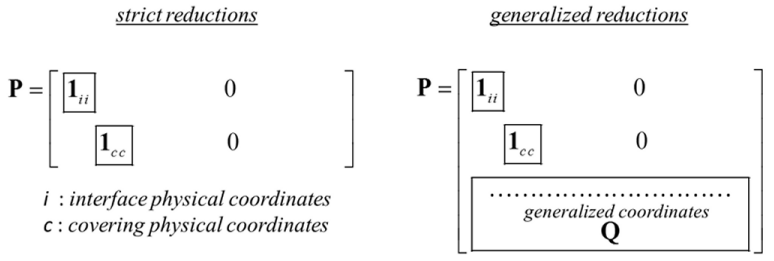

Figure 2. P-matrices associated with strict or generalized explicit coordinate reductions.

mechanical system governed by $\boldsymbol{k}$ and $\boldsymbol{m}$ reduced matrices. As illustrated in Figure 2 two types of reductions can be considered:

- *strict reductions* in ordinary physical coordinates, with unit diagonal blocks $\mathbf{1}_{ii}$ and $\mathbf{1}_{cc}$ inside the P-matrix, to localize interface coordinates, i, and supplementary "covering" ones, c, respectively;
- *generalized reductions*, where a P-matrix of the preceding type is augmented by supplementary rows expressing formal combinations of primary coordinates, i.e. generalized degrees of freedom corresponding to least-squares estimations, assumed vibration modes, or true eigenmodes.

The difference from one type of reduction to the other is not in obtaining dynamical stiffness relations, but in the assurance that a reasonable identification of a k-m system is possible. Primary coordinates have a clear physical meaning which makes that augmenting the set of covering coordinates necessarily implies convergence. Things are not so clear with generalized coordinates where the theoretical formulation of rules of convergence is a major issue in the construction of future solutions. It has been thought premature to introduce this problematic in the modeling of sandwich structures. Although the technique has already worked successfully with various generalized coordinates, the practical examples given in the paper have been limited to strict reductions.

Guyan reduction method will now serve to illustrate the "explicit" character of the considered approach. This method is given in the original paper [1] as a Ritz-Galerkin transformation based on the T-matrix

$$\boldsymbol{T}_{\text{Guyan}} = \begin{bmatrix} \mathbf{1}_{aa} \\ -\boldsymbol{K}_{dd}^{-1}\boldsymbol{K}_{da} \end{bmatrix}, \tag{3}$$

where a and d designate the coordinates to be retained or deleted, respectively. Unfortunately, as the choice of the T-matrix is only justified by the fact that it works correctly in Pure Statics, the method is termed a "static reduction", and the resulting formulae

$$\boldsymbol{k} = \boldsymbol{T}_{\text{Guyan}}^{T}\boldsymbol{K}\boldsymbol{T}_{\text{Guyan}} = \boldsymbol{K}_{aa} - \boldsymbol{K}_{ad}\boldsymbol{K}_{dd}^{-1}\boldsymbol{K}_{da}, \tag{4}$$

$$\boldsymbol{m} = \boldsymbol{T}_{\text{Guyan}}^{T}\boldsymbol{M}\boldsymbol{T}_{\text{Guyan}} = \boldsymbol{M}_{aa} - \boldsymbol{M}_{ad}\boldsymbol{K}_{dd}^{-1}\boldsymbol{K}_{da} - \boldsymbol{K}_{ad}\boldsymbol{K}_{dd}^{-1}\boldsymbol{M}_{da} + \boldsymbol{K}_{ad}\boldsymbol{K}_{dd}^{-1}\boldsymbol{M}_{dd}\boldsymbol{K}_{dd}^{-1}\boldsymbol{K}_{da} \tag{5}$$

are generally given as excellent for the stiffness but uncontrolled for the mass. Revisiting the Guyan reduction from the explicit point of view leads to consider a "Boolean" localization P-matrix of the form

$$\boldsymbol{P}_{\text{Guyan}} = \left[\mathbf{1}_{aa}\ \mathbf{0}_{ad}\right], \tag{6}$$

Equation (2) readily leads, through block-inversion, to what can be recognized as the exact expression of the reduced dynamic stiffness

$$\boldsymbol{\psi} = \left[\left(\boldsymbol{K}_{aa} - \omega^2\boldsymbol{M}_{aa}\right) - \left(\boldsymbol{K}_{ad} - \omega^2\boldsymbol{M}_{ad}\right)\left(\boldsymbol{K}_{dd} - \omega^2\boldsymbol{M}_{dd}\right)^{-1}\left(\boldsymbol{K}_{da} - \omega^2\boldsymbol{M}_{da}\right)\right]\boldsymbol{a}. \tag{7}$$

It then remains to proceed to a Taylor expansion at the origin with respect to $s = \omega^2$ to give back equations (4) and (5) (see details in [13]). From the explicit point of view, Guyan's formulae can thus be considered as true dynamic expressions. Apart from this, there is no reason why Ritz-Galerkin and explicit reductions should lead to identical results in all circumstances, as in the present example. The common root is rather to be found in the pseudo-inverse identity

$$\boldsymbol{P}_{\text{Guyan}} \times \boldsymbol{T}_{\text{Guyan}} = \mathbf{1}_{aa}, \tag{8}$$

which arises from equations (3) and (6).

2.2. Taylor-Laurent expansions

The global receptance term $(\boldsymbol{K} - \omega^2\boldsymbol{M})^{-1}$ in equation (2) is a function of the squared frequency $s = \omega^2$, that can be expanded at the origin in a series of the form

$$\left(\boldsymbol{K} - \omega^2\boldsymbol{M}\right)^{-1} = \boldsymbol{A}_0\omega^{-2} + \boldsymbol{A}_1\omega^0 + \boldsymbol{A}_2\omega^{-2} + \cdots + \boldsymbol{A}_p\omega^{2(p-1)} + \ldots \tag{9}$$

It results from direct algebraic considerations or, alternatively, from mode-superposition formulae of Appendix A4, that, according to whether the system is in fixed or in floating conditions, the expression is either a Taylor series, with $\boldsymbol{A}_0 = 0$, or a Laurent series, with a non-zero $\boldsymbol{A}_0$. Such series are convergent in frequency intervals $[0, \overline{\omega}]$, when $\boldsymbol{A}_0 = 0$, or $]0, \overline{\omega}]$, when $\boldsymbol{A}_0 \neq 0$, where $\overline{\omega}$ is less than the first non-zero eigenfrequency of the associated system. Because there is no direct relationship between the convergence of a given series and that of its inverse (think for example to $s = 1 - x$ and $s^{-1} = 1 + x + x^2 + \ldots$) Taylor-Laurent expansions of receptances can be used in Structural Dynamics, far beyond their effective radii of convergence, as pure *formal series* to study the inverse dynamic

stiffness. Mastering the formal mathematical relations between mass and stiffness matrices and the Taylor-Laurent coefficients can then be thought of as a possible way to adapt formula to effective structural reductions through the following three steps:

a. Expansion: formal Taylor-Laurent expansion (9) of dynamic receptance.

b. Reduction: reduction through the P-matrix

$$\begin{aligned} &\boldsymbol{P}\big(-\boldsymbol{A}_0\omega^{-2} + \boldsymbol{A}_1\omega^0 + \boldsymbol{A}_2\omega^2 \\ &\qquad + \cdots + \boldsymbol{A}_p\omega^{2(p-1)} + \ldots \big)\boldsymbol{P}^T \\ &= -\boldsymbol{a}_0\omega^{-2} + \boldsymbol{a}_1\omega^0 + \cdots + \boldsymbol{a}_p\omega^{2(p-1)} + \ldots \end{aligned} \tag{10}$$

c. Retrieval: retrieval of reduced $\boldsymbol{k}$ and $\boldsymbol{m}$ matrices through (approximate) identification

$$\begin{aligned} &\big(-\boldsymbol{a}_0\omega^{-2} + \boldsymbol{a}_1\omega^0 + \cdots + \boldsymbol{a}_p\omega^{2(p-1)} + \ldots \big)^{-1} \\ &\qquad \big(\boldsymbol{k} - \boldsymbol{m}\omega^2\big) = \boldsymbol{1}. \end{aligned} \tag{11}$$

3. Taylor reduction of fixed systems

3.1. Preliminaries

In fixed conditions of analysis, $\boldsymbol{K}$ and $\boldsymbol{M}$ are symmetric, strictly positive and thus invertible $N \times N$ matrices. The global receptance can then be expanded in a Taylor series

$$\begin{aligned} &\big(\boldsymbol{K} - \omega^2\boldsymbol{M}\big)^{-1} = \\ &\quad \boldsymbol{A}_1\omega^0 + \boldsymbol{A}_2\omega^2 + \cdots + \boldsymbol{A}_p\omega^{2(p-1)} + \ldots \end{aligned} \tag{12}$$

The question now is to calculate the corresponding coefficients.

3.2. Expansion

The identification of Taylor coefficients relative to the global receptance starts with

$$\begin{aligned} &\big(\boldsymbol{K} - \omega^2\boldsymbol{M}\big)\big(\boldsymbol{0} + \boldsymbol{A}_1\omega^0 + \boldsymbol{A}_2\omega^2 \\ &\qquad + \cdots + \boldsymbol{A}_p\omega^{2(p-1)} + \ldots \big) = \boldsymbol{1}. \end{aligned} \tag{13}$$

Setting to zero successive terms in the development

$$\begin{aligned} &\big(\boldsymbol{K}\boldsymbol{A}_1 - \boldsymbol{1}\big)\omega^0 + \big(\boldsymbol{K}\boldsymbol{A}_2 - \boldsymbol{M}\boldsymbol{A}_1\big)\omega^2 \\ &+ \cdots + \big(\boldsymbol{K}\boldsymbol{A}_{p+1} - \boldsymbol{M}\boldsymbol{A}_p\big)\omega^{2p} + \ldots = \boldsymbol{0} \end{aligned} \tag{14}$$

readily yields the following solution to the problem

$$\boldsymbol{A}_1 = \boldsymbol{K}^{-1}, \tag{15}$$

$$\boldsymbol{A}_p = \boldsymbol{K}^{-1}\boldsymbol{M}\boldsymbol{A}_{p-1} \text{ for every } p \geq 2, \tag{16}$$

or, because the terms in equations (16) form a geometric matrix progression

$$\boldsymbol{A}_p = \boldsymbol{\Lambda}^{p-1}\boldsymbol{A}_1 \quad \text{for every } p \geq 2, \text{ with } \boldsymbol{\Lambda} = \boldsymbol{K}^{-1}\boldsymbol{M}. \tag{17}$$

3.3. Contraction

It results from the preceding analysis that Taylor coefficients $\boldsymbol{A}_p$ are invertible matrices. A point of capital importance for the following is that, just after reduction, reduced coefficients $\boldsymbol{a}_p = \boldsymbol{P}\boldsymbol{A}_p\boldsymbol{P}^T$ are still invertible matrices. As a matter of fact, in pure reductions of the Guyan type, with $\boldsymbol{P} = [\boldsymbol{1}_{aa}\ \boldsymbol{0}_{ad}]$ a $n \times N$ localization matrix, reduced coefficients are just diagonal blocks of invertible global coefficients. In generalized reductions, it is shown in Appendix A4 that this property remains true provided matrix $\boldsymbol{P}$ has linearly independent rows corresponding to independent generalized coordinates.

3.4. Retrieval

As a principle of approximation, the subsystem inside the fixed system may be considered as being very close to an autonomous fixed system. By itself, this hypothesis is nothing exceptional, since it will automatically hold if a sufficient number of degrees of freedom are retained in the condensation set. This leads to transform, in some approximate sense, equations (13) to (17), relative to the overall system, into equivalent equations relative to reduced $\boldsymbol{a}_p$ and unknown $\boldsymbol{k}$ and $\boldsymbol{m}$. Among all the possible strategies of identification, the invertibility of $\boldsymbol{a}_p$ means that, regardless of high order coefficients $\boldsymbol{a}_p$, $p \geq 2$ it is possible to focus on the leading terms

$$\boldsymbol{a}_1 = \boldsymbol{k}^{-1}, \tag{18}$$

$$\boldsymbol{a}_2 = \boldsymbol{k}^{-1}\boldsymbol{m}\boldsymbol{a}_1 \tag{19}$$

to express finally the reduced mass and stiffness matrices as

$$\boldsymbol{k} = \boldsymbol{a}_1^{-1}, \tag{20}$$

$$\boldsymbol{m} = \boldsymbol{a}_1^{-1}\boldsymbol{a}_2\boldsymbol{a}_1^{-1} = \boldsymbol{k}\boldsymbol{a}_2\boldsymbol{k}. \tag{21}$$

3.5. Conclusion

In principle, the computation is limited to the first two Taylor coefficients and can be schematically viewed as indicated in Figure 3. In practice, the expansion and contraction steps can be combined to avoid the inversion of $\boldsymbol{K}$ and the explicit computation of full global Taylor coefficients. It is indeed possible to compute two auxiliary $N \times n$ matrices -$\boldsymbol{y}_1 = \boldsymbol{A}_1\boldsymbol{P}^T$ and $\boldsymbol{y}_2 = \boldsymbol{A}_2\boldsymbol{P}^T$- by solving two nested parallel systems with n second members -$\boldsymbol{K}\boldsymbol{y}_1 = \boldsymbol{P}^T$, $\boldsymbol{K}\boldsymbol{y}_2 = \boldsymbol{M}\boldsymbol{y}_1$- and then write reduced coefficients as $\boldsymbol{a}_1 = \boldsymbol{P}\boldsymbol{y}_1$ and $\boldsymbol{a}_2 = \boldsymbol{P}\boldsymbol{y}_2$.

It should be noted that this technique of approximation consists basically in keeping the two leading terms in the Taylor expansion of relation (7). Although it is not obvious, when comparing formulae (15) to (21) with Guyan's expressions (4) and (5), it should be clear that the two methods lead to absolutely identical results, as far as strict reductions are considered. The explicit method is in this case a block decomposition of Guyan's approach. Its main advantage is that it also works with generalized coordinates. Moreover, it clearly opens the way to unexplored

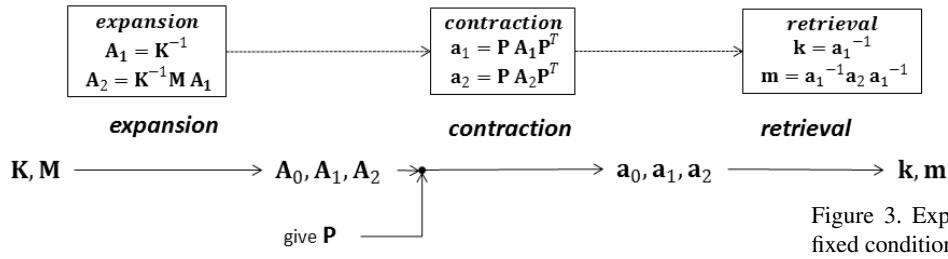

Figure 3. Explicit coordinate reduction in fixed conditions of analysis.

possibilities of estimating errors and frequency bandwidth by examining, for example, the divergence of the series of the reduced coefficients $\boldsymbol{a}_p$ to the geometric Taylor series, $\tilde{\boldsymbol{a}}_p = (\boldsymbol{k}^{-1}\boldsymbol{m})^{p-1}\boldsymbol{a}_1$, which can be attached to the reduced system by a mere transposition of equations (15), (16) and (17).

4. "Covering-censoring" reduction of free-floating systems

4.1. Introduction

Fixed conditions are much easier to handle than free-floating ones but are of less practical interest in model reduction since letting condensed matrices depend on an implicit freezing of some kinematic variables clearly hinders the use of such matrices. Thus, the theory must now be developed in free-floating conditions, with two major difficulties: the singularity of matrix $\boldsymbol{K}$ imposes the use of pseudo-inverse formulae (Appendix), and reduced Laurent coefficients in free-floating conditions being neither those of a fixed system nor those of a free-floating one, the operations of contraction and retrieval must be carefully redefined.

In free-floating conditions of analysis, $\boldsymbol{M}$ is, as before, a symmetric positive definite $N \times N$ matrix but $\boldsymbol{K}$ is a symmetric semi-positive $N \times N$ matrix. The kernel, or nullspace, of $\boldsymbol{K}$, defined as $\ker\boldsymbol{K} = \{\boldsymbol{x}|\boldsymbol{K}\boldsymbol{x} = 0\}$, is now a non-empty vector space of dimension $\sigma > 0$ associated with "stress-free motions" i.e. (in most common engineering applications) with a set of dimension $\sigma = 6$ of rigid body motions. It is convenient to introduce a $N \times \sigma$ "spanning matrix", $\boldsymbol{S}$, whose columns form the basis of $\ker\boldsymbol{K}$, which will be denoted $\ker\boldsymbol{K} = ((\boldsymbol{S}))$. The range or image of $\boldsymbol{K}$ is defined as $\mathrm{range}\boldsymbol{K} = \{\boldsymbol{f}|\exists\boldsymbol{x}, \boldsymbol{f} = \boldsymbol{K}\boldsymbol{x}\}$. The dimension of this subspace, termed the rank of $\boldsymbol{K}$, is denoted $\mathrm{rank}\boldsymbol{K}$. For the stiffness matrices considered, this notion refers to the distributions of nodal forces that can be effectively developed by the system, and is clearly strongly connected with the ability to develop or not strain-free motions. According to a quite classical theorem of Linear Algebra given in Appendix A1 as "Lagrange lemma", $\mathrm{range}\boldsymbol{K}$ is the collection, $(\ker\boldsymbol{K})^{\perp}$, of all vectors orthogonal to $\ker\boldsymbol{K}$ while, conversely, $\ker\boldsymbol{K}$ is the collection, $(\mathrm{range}\boldsymbol{K})^{\perp}$, of all vectors orthogonal to $\mathrm{range}\boldsymbol{K}$. With the usual primal-dual identification $E \equiv E' \equiv R^N$, $\ker\boldsymbol{K}$ and $\mathrm{range}\boldsymbol{K}$ can be given as *orthogonal complementary subspaces* satisfying $\mathrm{range}\boldsymbol{K} \perp \ker\boldsymbol{K}$ and $\mathrm{range}\boldsymbol{K} \oplus \ker\boldsymbol{K} = \mathbf{R}^N$. Consequently, $\mathrm{rank}\boldsymbol{K} = N - \sigma$. Moreover, every element $\boldsymbol{f}$ of $\mathrm{range}\boldsymbol{K}$, i.e. every admissible distribution of nodal forces, must satisfy $\boldsymbol{S}^T\boldsymbol{f} = 0$ or, in other words, must be a self-equilibrated system of forces.

4.2. Expansion

Owing to the singularity of $\boldsymbol{K}$, the Taylor expansion of the preceding section is now replaced by a Laurent series, with $\boldsymbol{A}_0 \neq 0$. Laurent coefficients can be identified through

$$\begin{aligned}\big(\boldsymbol{K} - \omega^2\boldsymbol{M}\big)\big(- \boldsymbol{A}_0\omega^{-2} + \boldsymbol{A}_1\omega^0 + \boldsymbol{A}_2\omega^2 \\ + \cdots + \boldsymbol{A}_p\omega^{2(p-1)} + \ldots\big) = \mathbf{1}.\end{aligned} \tag{22}$$

Setting to zero the successive terms in the development

$$\begin{aligned}\big(- \boldsymbol{K}\boldsymbol{A}_0\big)\omega^{-2} + \big(\boldsymbol{K}\boldsymbol{A}_1 + \boldsymbol{M}\boldsymbol{A}_0 - \mathbf{1}\big)\omega^0 \\ + \big(\boldsymbol{K}\boldsymbol{A}_2 - \boldsymbol{M}\boldsymbol{A}_1\big)\omega^2 + \ldots \\ + \big(\boldsymbol{K}\boldsymbol{A}_{p+1} - \boldsymbol{M}\boldsymbol{A}_p\big)\omega^{2p} + \ldots = \mathbf{0}\end{aligned} \tag{23}$$

now involves a cascade of pseudo-inversions. One can find in Appendix A3 how Laurent coefficients can be determined using adequate techniques of Singular Linear Algebra which are detailed in Appendices A1 and A2. This apparently purely mathematical method is, in the authors' opinion, the only one to approach the intricate physical notions of "inertial", "inertia relief" and "elastic" displacements or modes efficiently and correctly. The method brings out a complete generalization of relations (15) and (16), which can now be written

$$\boldsymbol{A}_0 = \boldsymbol{S}\big(\boldsymbol{S}^T\boldsymbol{M}\boldsymbol{S}\big)^{-1}\boldsymbol{S}^T, \tag{24}$$

$$\boldsymbol{A}_1 = \big(\mathbf{1} - \boldsymbol{\Pi}_M\big)\big(\lambda\boldsymbol{\Pi} + \boldsymbol{K}\big)^{-1}\big(\mathbf{1} - \boldsymbol{\Pi}_M^T\big), \tag{25}$$

$$\forall p \geq 2,\ \boldsymbol{A}_p = \boldsymbol{\Lambda}^{p-1}\boldsymbol{A}_1 \text{ with}$$

$$\boldsymbol{\Lambda} = \big(\mathbf{1} - \boldsymbol{\Pi}_M\big)\big(\lambda\boldsymbol{\Pi} + \boldsymbol{K}\big)^{-1}\boldsymbol{M}, \tag{26}$$

where, according to Appendices A1 and A2

- $\boldsymbol{\Pi} = \boldsymbol{S}(\boldsymbol{S}^T\boldsymbol{S})^{-1}\boldsymbol{S}^T$ is the orthogonal projector on $\ker\boldsymbol{K}$;
- $\boldsymbol{\Pi}_M = \boldsymbol{S}(\boldsymbol{S}^T\boldsymbol{M}\boldsymbol{S})^{-1}\boldsymbol{S}^T\boldsymbol{M}$ is the projector on $\ker\boldsymbol{K}$ relative to the $\boldsymbol{M}$-metric;
- $(\lambda\boldsymbol{\Pi} + \boldsymbol{K})^{-1}$, with λ an arbitrary non-zero number, is an expression of the SVD pseudo-inverse of $\boldsymbol{K}$.

Analyzing the singularity of Laurent coefficients is the key to the retrieval of structural matrices. The analysis is carried out in Appendix A4 and leads to the following results

$$\text{range}\boldsymbol{A}_0 = \big((\boldsymbol{S})\big), \tag{27}$$

$$\text{range}\boldsymbol{A}_p = \big((\boldsymbol{MS})\big)^{\perp} \text{ for each } p \geq 1. \tag{28}$$

4.3. Contraction

4.3.1. Basic observations

The whole complexity and interest of the Laurent free-floating reduction lies in the fact that, immediately after contraction through the $n \times N$ P-matrix, the reduced coefficients correspond to neither a fixed nor a free-floating system. It is indeed shown in Appendix A4 that

$$\text{range}\hat{\boldsymbol{a}}_0 = \big((\boldsymbol{PS})\big), \tag{29}$$

$$\text{range}\hat{\boldsymbol{a}}_p = n \text{ for each } p \geq 1. \tag{30}$$

Coefficients $\hat{\boldsymbol{a}}_p$ are thus improper to any coherent identification of $\boldsymbol{k}$ and $\boldsymbol{m}$ matrices. Far from being a deadlock, this odd particularity - in close connection with the modeling of internal interactions evoked at the beginning of the paper- constitutes the main advantage of the reductions in free-floating conditions.

Relations (28) and (30) have a quite universal significance concerning all possible systems and embedded subsystems, which can be enounced as follows:

> **Degeneracy theorem**- *In free-floating conditions of analysis, regularity of reduced Laurent coefficients of order $p > 0$ is the rule for all strict subsystems, while singularity of Laurent coefficients of order $p > 0$ is the distinguishing mark of all autonomous systems.*

As a consequence, apparition during an explicit reduction of ill-conditioning in Laurent coefficients is the distinguishing mark that the condensation set makes closer to an autonomous free-floating system, provided ill-conditioning is not artificially due to the introduction of linear dependencies in the P-matrix. Conversely, a progressive degeneracy will be necessarily observed, for example when, during a strict reduction, the condensation set tends to cover the whole initial system. Unlike what happens in fixed conditions of analysis, convergence of the reduction becomes detectable and a new strategy begins to stand out, involving

i) a "covering" phase, during which matrix P is augmented until degeneracy appears in the spectrum of coefficients $\hat{\boldsymbol{a}}_p$, $p > 0$;

ii) a "censoring" phase consisting, once the proximity to an autonomous free-floating system has been detected, in a slight transformation of raw coefficients , $\hat{\boldsymbol{a}}_p$, $p > 0$, in neighboring singular coefficients, $\boldsymbol{a}_p$, supposed to represent the detected free-floating system (this phase is termed "censoring" because it roughly consists in setting to zero the lowest eigenvalues of $\hat{\boldsymbol{a}}_p$, which is the simplest method to produce singular matrices in the close vicinity of regular ones);

iii) a "retrieval" phase, consisting in the reverse identification of $\boldsymbol{k}$ and $\boldsymbol{m}$ matrices, as in fixed conditions of analysis, but using the singular formulae of Appendix A3.

4.3.2. Precise rules of reduction

First, it should be noted that equation (29) describes exactly the set of reduced stress-free motions that should be observed after reduction through the P-matrix. Coefficient $\hat{\boldsymbol{a}}_0$ is thus to be retained in without any modification or censoring. From this, the reduced dimension

$$\hat{\sigma} = \dim\big((\boldsymbol{PS})\big), \tag{31}$$

which fixes the rank of the matrix, $\boldsymbol{k}$, to be identified, can be given as a number of capital importance in the precise definition of operations. Indeed transposing relations (28) and (29) from the initial free-floating system to the current reduced one leads to

$$\text{range}\hat{\boldsymbol{a}}_0 = \big((\boldsymbol{s})\big) \equiv \big((\boldsymbol{PS})\big), \tag{32}$$

$$\text{range}\hat{\boldsymbol{a}}_p = \big((\boldsymbol{ms})\big)^{\perp} \text{ for each } p \geq 1, \tag{33}$$

with the clear consequence that coherent censored coefficients must satisfy

$$\text{rank}\boldsymbol{a}_p = n - \hat{\sigma} \text{ for each } p \geq 1, \tag{34}$$

Thus, it can be concluded that

i) censoring can be precisely defined as setting to zero, after diagonalization, the $\hat{\sigma}$ lowest eigenvalues of raw coefficients according to the following scheme:

$$\hat{\boldsymbol{a}}_p = \boldsymbol{U}^T \text{diag}\big\{\lambda_1, \ldots, \lambda_\sigma, \lambda_{\sigma+1}, \ldots, \lambda_n\big\}\boldsymbol{U} \tag{35}$$
$$\xrightarrow[\text{censoring}]{} \boldsymbol{a}_p = \boldsymbol{U}^T \text{diag}\big\{0, \ldots, 0, \lambda_{\sigma+1}, \ldots, \lambda_n\big\}\boldsymbol{U}.$$

ii) spectral inspection during the covering phase can be precisely defined as the detection of a gap from the $\hat{\sigma}$ lowest eigenvalues to the others.

In addition, equation (34) shows that identifying $\boldsymbol{k}$ and $\boldsymbol{m}$ matrices from $\hat{\boldsymbol{a}}_0$, $\boldsymbol{a}_1$ and $\boldsymbol{a}_2$ coefficients, regardless of higher order coefficients, is the best which can be done since it amounts to draw $n - \sigma + n = 2n - \sigma$ independent columns from $\sigma + n - \sigma + n - \sigma = 2n - \sigma$ other independent columns. Thus, only $\hat{\boldsymbol{a}}_1$ and $\hat{\boldsymbol{a}}_2$ are concerned by the spectral inspection and censoring and only $\hat{\boldsymbol{a}}_0$, $\boldsymbol{a}_1$ and $\boldsymbol{a}_2$ are concerned by the final retrieval step.

4.4. Retrieval

4.4.1. Preparation

Transposing the constitutive relations obtained in §4.2 for the initial free-floating system to the inertial reduced coefficient, $\boldsymbol{a}_0 = \hat{\boldsymbol{a}}_0$, and to the censored reduced coefficients, $\boldsymbol{a}_1$ and $\boldsymbol{a}_2$ is the key to retrieve the reduced matrices $\boldsymbol{k}$ and $\boldsymbol{m}$. This leads first to introduce, as an intermediate variable, a spanning matrix $\boldsymbol{s}$ such that

$$\text{ker}\boldsymbol{k} = \big((\boldsymbol{s})\big). \tag{36}$$

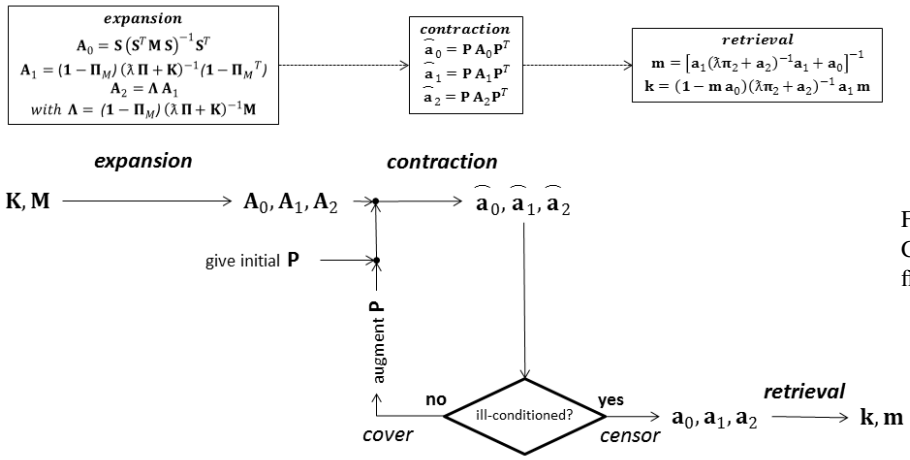

Figure 4. Explicit "Covering-Censoring" Reduction in free-floating conditions of analysis.

From this, the following structural relations are directly inherited from equations (27) and (28):

$$\ker\boldsymbol{a}_0 = \big((\boldsymbol{s})\big)^{\perp}, \tag{37}$$

$$\ker\boldsymbol{a}_1 = \big((\boldsymbol{ms})\big), \tag{38}$$

$$\ker\boldsymbol{a}_2 = \big((\boldsymbol{ms})\big). \tag{39}$$

Identification relations (23) can also be transposed, leading to (in a symmetric form, to facilitate the identification)

$$\boldsymbol{a}_0 = \boldsymbol{s}\big(\boldsymbol{s}^T\boldsymbol{ms}\big)^{-1}\boldsymbol{s}^T, \tag{40}$$

$$\boldsymbol{a}_1\boldsymbol{k} + \boldsymbol{a}_0\boldsymbol{m} = \mathbf{1}, \tag{41}$$

$$\boldsymbol{a}_2\boldsymbol{k} - \boldsymbol{a}_1\boldsymbol{m} = \mathbf{0}. \tag{42}$$

4.4.2. Identification of $\boldsymbol{m}$

Matrix $\boldsymbol{m}$ may be assumed to be invertible, and equations (41) and (42) can be rewritten as

$$\boldsymbol{a}_1\boldsymbol{k}\boldsymbol{m}^{-1} = \boldsymbol{m}^{-1} - \boldsymbol{a}_0, \tag{43}$$

$$\boldsymbol{a}_2\boldsymbol{k}\boldsymbol{m}^{-1} - \boldsymbol{a}_1 = \mathbf{0}. \tag{44}$$

From the SVD pseudo-inverse theorem of Appendix A2, equations (44) and (39) give the following general expression of $\boldsymbol{k}\boldsymbol{m}^{-1}$,

$$\boldsymbol{k}\boldsymbol{m}^{-1} = \big(\lambda\pi_2 + \boldsymbol{a}_2\big)^{-1}\boldsymbol{a}_1 + \boldsymbol{ms}\boldsymbol{\alpha}, \tag{45}$$

where π_2 designates the orthogonal projector onto $\ker\boldsymbol{k}$; λ, an arbitrary non-zero number; and $\boldsymbol{\alpha}$ an auxiliary matrix variable.

Since, from condition (38), every term in the form of $\boldsymbol{ms}\boldsymbol{\alpha}$ is known to lie in $\ker\boldsymbol{a}_1$, one may infer using equation (45) that

$$\boldsymbol{a}_1\boldsymbol{k}\boldsymbol{m}^{-1} = \boldsymbol{a}_1\big(\lambda\pi_2 + \boldsymbol{a}_2\big)^{-1}\boldsymbol{a}_1. \tag{46}$$

Equation (43) then gives

$$\boldsymbol{a}_1\big(\lambda\pi_2 + \boldsymbol{a}_2\big)^{-1}\boldsymbol{a}_1 = \boldsymbol{m}^{-1} - \boldsymbol{a}_0. \tag{47}$$

There is no difficulty at this stage to draw from the latter equation the final expression of $\boldsymbol{m}$ as

$$\boldsymbol{m} = \left[\boldsymbol{a}_0 + \boldsymbol{a}_1\big(\lambda\pi_2 + \boldsymbol{a}_2\big)^{-1}\boldsymbol{a}_1\right]^{-1}. \tag{48}$$

4.4.3. Identification of $\boldsymbol{k}$

Knowing matrix $\boldsymbol{m}$ and assigning a precise value to $\boldsymbol{\alpha}$ in equation (45) can give a possible expression for $\boldsymbol{k}$. Multiplying this equation by $\boldsymbol{s}^T$ and because $\boldsymbol{ks} = 0$, leads to

$$\mathbf{0} = \boldsymbol{s}^T\big(\lambda\pi_2 + \boldsymbol{a}_2\big)^{-1}\boldsymbol{a}_1 + \boldsymbol{s}^T\boldsymbol{ms}\boldsymbol{\alpha}. \tag{49}$$

A first expression of $\boldsymbol{\alpha}$ is thus given by

$$\boldsymbol{\alpha} = -\big(\boldsymbol{s}^T\boldsymbol{ms}\big)^{-1}\boldsymbol{s}^T\big(\lambda\pi_2 + \boldsymbol{a}_2\big)^{-1}\boldsymbol{a}_1. \tag{50}$$

Substituting the expression of $\boldsymbol{\alpha}$ into equation (45) and multiplying the resulting equation by $\boldsymbol{m}$ on the right, gives then $\boldsymbol{k}$ as

$$\begin{aligned}\boldsymbol{k} = {} & \big(\lambda\pi_2 + \boldsymbol{a}_2\big)^{-1}\boldsymbol{a}_1\boldsymbol{m} \\ & - \boldsymbol{ms}\big(\boldsymbol{s}^T\boldsymbol{ms}\big)^{-1}\boldsymbol{s}^T\big(\lambda\pi_2 + \boldsymbol{a}_2\big)^{-1}\boldsymbol{a}_1\boldsymbol{m}.\end{aligned} \tag{51}$$

This expression, by equation (40), is equivalent to

$$\begin{aligned}\boldsymbol{k} = {} & \big(\lambda\pi_2 + \boldsymbol{a}_2\big)^{-1}\boldsymbol{a}_1\boldsymbol{m} \\ & - \boldsymbol{m}\boldsymbol{a}_0\big(\lambda\pi_2 + \boldsymbol{a}_2\big)^{-1}\boldsymbol{a}_1\boldsymbol{m}.\end{aligned} \tag{52}$$

After factorization, the expression of $\boldsymbol{k}$ is given, in terms of the reduced censored Laurent coefficients and the mass matrix of equation (48), by

$$\boldsymbol{k} = \big(1 - \boldsymbol{m}\boldsymbol{a}_0\big)\big(\lambda\pi_2 + \boldsymbol{a}_2\big)^{-1}\boldsymbol{a}_1\boldsymbol{m}. \tag{53}$$

4.5. Conclusion

Equations (48) and (53) complete the identification of the reduced $\boldsymbol{m}$ and $\boldsymbol{k}$ matrices. The overall scheme of reduction, termed "Explicit Covering-Censoring Reduction", is outlined in Figure 4. In practice, explicit computations of full overall Taylor coefficients can be avoided using the technique described in §3.5 for fixed conditions of analysis. This method also shares the general properties observed in fixed conditions concerning the possible extensions to generalized coordinates. The domain of application is wider than Guyan reductions: Guyan technique,

for example, cannot be applied to the reductions of plate models to normal deflections and rotations which are presented in sections 5 and 6 for the very reason that in each case, block $\boldsymbol{K}_{dd}$ in equation (4) is not invertible. Checking the quality of reduction using a criterion on characteristic eigenvalues is the most striking feature of the method, that spares, if not the reduction itself (since most of the work is done when Laurent coefficients are at disposal), but a lot of unnecessary comparisons of FRF's before and after reduction. Estimation of errors and frequency bandwidths should be drawn from the study of the remainders of Laurent series, which could consist, for example, in measuring the divergence of the series of reduced coefficients $\hat{\boldsymbol{a}}_p$ to the geometric Laurent series, $\hat{\boldsymbol{a}}_p = [(1 - \boldsymbol{\pi}_m)(\lambda\boldsymbol{\pi} + \boldsymbol{k})^{-1}\boldsymbol{m}]\boldsymbol{a}_1$, which can be attached to the reduced system by a transposition of equations (25) and (26).

5. Reduction of sandwich plate models

5.1. Introduction

In the finite element implementation of layer-wise theories for multilayered structures, such as laminate and sandwich structures, condensation techniques are often required to switch from the description of multilayer to equivalent single layer variables (see for instance [27]). This is also the case in displacement-stress hybrid formulations where the stress unknowns are eliminated, by means of a static condensation technique, to keep only the displacements as nodal variables [28]. In the following, the reduction method presented above is used to eliminate specific variables in a layer-wise model for the analysis of viscoelastically damped sandwich plates. First, the sandwich finite element formulation is described. This formulation leads to a triangular finite element with seven dofs per node. Then, the reduction method is used to reduce the model to the classical three dofs per node for homogeneous bending plates.

5.2. Sandwich plate model

The finite element formulation is taken from [20]. The faces of the sandwich plate are assumed to be thin and to resist membrane and bending stresses only (Kirchhoff's theory), whereas the core can resist membrane, bending and shear stresses (Mindlin's theory). The displacement field satisfies the following hypotheses: (1) normal sections in each layer before deformation remain plane and continuous after deformation; (2) the transverse displacement remains constant throughout the thickness of the plate; (3) the face-layers are elastic and isotropic and are subjected to extension, bending and in-plane shear deformations; (4) the core is subjected to extension, bending, in-plane shear deformations and transverse shear deformations; (5) all displacements are assumed to be small and continuous at the interfaces.

A more precise kinematic description can now be given using a Cartesian system of coordinates (x, y, z), whose origin is in the mid-plane of the core while axis z lies along the normal to the plate as shown in Figure 5. Now denoting

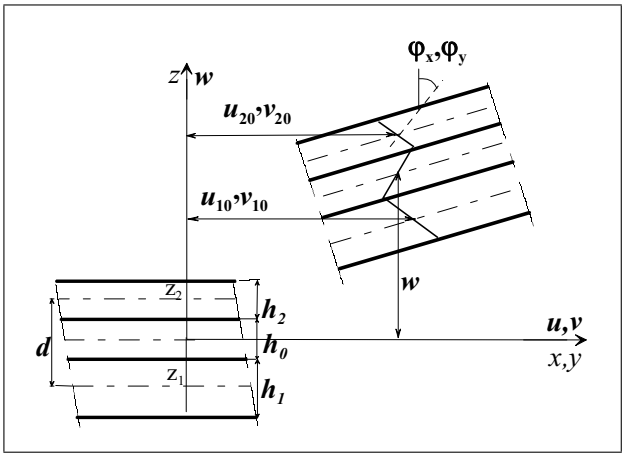

Figure 5. Kinematics of the sandwich plate model.

- $\varphi_x = u_r/h_0 + (d/h_0 - 1)w_{,x}$ and $\varphi_y = v_r/h_0 + (d/h_0 - 1)w_{,y}$, the shear rotations of the normal to the core mid-plane;
- u_m, v_m, the mean mid-plane displacements defined by $u_m = (u_{10} + u_{20})/2$, $v_m = (v_{10} + v_{20})/2$ where $u_{\alpha 0}$, $v_{\alpha 0}$ $\alpha = 1, 2$, denote the in-plane displacements of the mid-surfaces of the top and bottom faces;
- u_r, v_r, the relative mid-plane displacements, $u_r = u_{10} - u_{20}$, $v_r = v_{10} - v_{20}$;

one can define the resulting piecewise-linear displacement, as shown in Table I, where z_α, $\alpha = 1, 2$, are the z coordinates of face mid-planes; $z_m = (z_1 + z_2)/2$ is the mean coordinate; $d = z_1 - z_2$ is the distance between the mid-planes of the faces; and h_1, h_2, h_0 are the thicknesses of the face-layers and of the core. The in-plane strain and stress fields in each layer and the transverse shear strain and stress fields in the core can be determined through standard displacement-strain and strain-stress relationships. Then, the strain and kinetic energies of the sandwich plate are expressed in terms of the mean mid-plane displacements of the faces u_m, v_m; the relative mid-plane displacements u_r, v_r; and the transverse deflection w. The approximate stiffness and mass matrices are then obtained from a specific two-dimensional 3-node plate element [20] having seven degrees of freedom per node, and performing linear interpolations of the membrane displacements u_m, v_m, u_r and v_r, and cubic interpolations of the bending displacements w, $w_{,x}$, $w_{,y}$. For viscoelastically damped sandwich plates, the damping is introduced through the elastic-viscoelastic correspondence principle, which amounts to changing real stiffness matrices into complex ones [29].

5.3. Construction of the reduced model

The Covering-Censoring reduction method is used to derive the reduced stiffness and mass matrices, starting from the initial undamped stiffness matrix $\boldsymbol{K}$ and mass matrix $\boldsymbol{M}$ of the sandwich plate. Then, the damping characteristics are introduced in the reduced model by changing the stiffness matrix $\boldsymbol{k}$ to $\hat{\boldsymbol{k}} = [1+\mathrm{i}\eta(\omega)]\boldsymbol{k}$. The loss factor $\eta(\omega)$

Table I. Displacement field in the sandwich plate.

layers	x-displacement	y-displacement	z-displacement
top	$u_m + \frac{1}{2}u_r + (z - z_1)w_{,x}$	$v_m + \frac{1}{2}v_r + (z - z_1)w_{,y}$	$w(x,y)$
core	$u_m + z_m w_{,x} + z\varphi_x$	$v_m + z_m w_{,y} + z\varphi_y$	
bottom	$u_m - \frac{1}{2}u_r + (z - z_2)w_{,x}$	$v_m - \frac{1}{2}v_r + (z - z_2)w_{,y}$	

can be estimated using the Modal Strain Energy (MSE) method [22, 23]. Indeed, this method states that, for a given undamped vibration mode, the ratio of the sandwich plate loss factor to the viscoelastic material loss factor can be estimated as the ratio of the elastic strain energy in the core to the total elastic energy in the sandwich plate. One thus writes

$$\frac{\eta_m}{\eta_v} = \frac{U_v^{(m)}}{U_s^{(m)}}, \tag{54}$$

where η_m is the modal loss factor associated to the m'th mode shape $\boldsymbol{\psi}$; η_v is the loss factor of the core material; $U_v^{(m)}$ and $U_s^{(m)}$ are the elastic strain energies for the mth mode shape, inside the core and the sandwich structure, respectively. As the damping is neglected in the faces, the complex stiffness matrix of the sandwich plate can be decomposed as

$$\boldsymbol{K} = \boldsymbol{K}_f + \left(1 + \mathrm{i}\eta_v\right)\boldsymbol{K}_v = \boldsymbol{K}^R + \mathrm{i}\boldsymbol{K}^I, \tag{55}$$

Where $\boldsymbol{K}_f$ and $\boldsymbol{K}_v$ are the elastic stiffness matrices of the faces and of the core, respectively. The modal loss factors can thus be computed as

$$\eta_m = \eta_v \frac{U_v^{(m)}}{U_s^{(m)}} = \eta_v \frac{\boldsymbol{\psi}_m^T \boldsymbol{K}_v \boldsymbol{\psi}_m}{\boldsymbol{\psi}_m^T \boldsymbol{K}^R \boldsymbol{\psi}_m} = \frac{\boldsymbol{\psi}_m^T \boldsymbol{K}^I \boldsymbol{\psi}_m}{\boldsymbol{\psi}_m^T \boldsymbol{K}^R \boldsymbol{\psi}_m}. \tag{56}$$

Defining a continuous interpolation such that $\eta(\omega_m) = \eta_m$ gives the expression of $\eta(\omega)$.

It should be noticed that the viscoelastic material properties vary significantly with temperature and frequency. To take these variations into account, the eigenvalue problem to obtain the eigenfrequencies and associated mode shapes must be solved using an iterative procedure as described in Figure 6 [30, 31]. First, the properties of the viscoelastic material can be determined at the first modal frequency of the structure without the damping layer. The complex modulus properties of commonly available damping materials as a function of temperature and frequency can be obtained using temperature-frequency nomograms supplied by the manufacturers [29]. Then, after the eigenvalue problem has been solved, the viscoelastic material properties are updated using the new frequency obtained. This process is repeated until the convergence between the value of the frequency used for calculating the damping material properties and the particular frequency is attained with an error of less than 1%. The process is expected to converge after a few iterations.

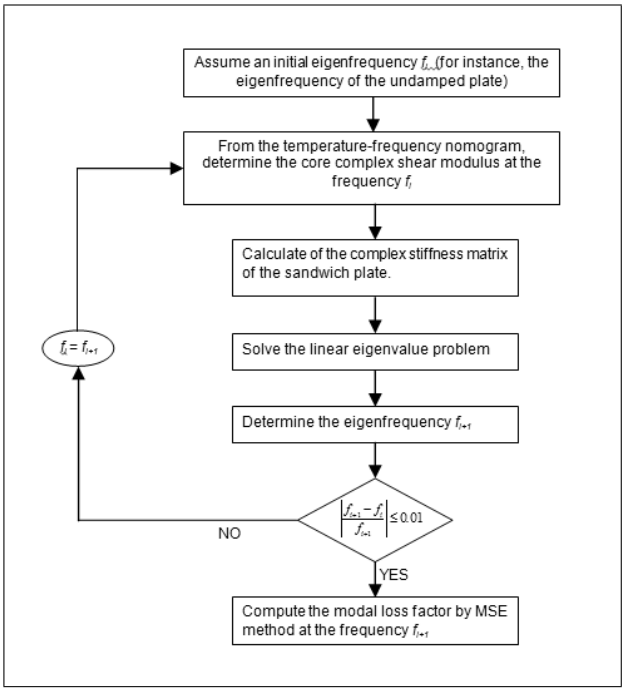

Figure 6. Flow-chart of the modal loss factor computation.

5.4. Test example

In the following, an application of the preceding method to the reduction of a finite element sandwich plate model is presented. The plate is 297 mm long, 210 mm wide with thicknesses of 3 mm for the base plate, 0.5 mm for the constraining layer, and 1 mm for the viscoelastic layer. The material properties are given in Table II. The plate is modeled by a relatively coarse mesh of 48 triangular sandwich elements, 35 nodes and a total of 245 dofs as shown in Figure 7. Various model reductions are performed:

1) a 10/245 reduction to the transverse displacement, w, at nodes 1 to 10;

2) a 35/245 reduction to the transverse displacement, w, at nodes 1 to 35;

3) a 105/245 reduction to the transverse displacement and rotations, w, w_x, w_y, at nodes 1 to 35.

Figure 8 shows the spectrum of Laurent-coefficient $\hat{\boldsymbol{a}}_2$ for each of the preceding reduction. The decay in the conditioning is quite spectacular, and illustrates what was expected in the theoretical section. It should be noted that a gap, marked with a plain arrow, appears between the third

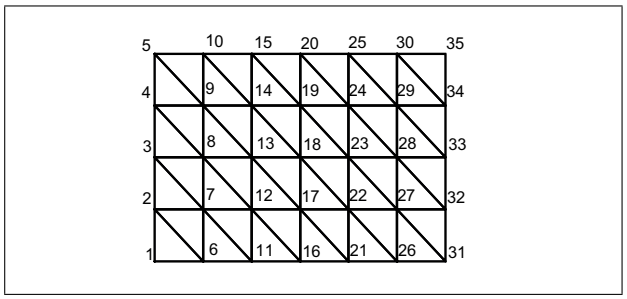

Figure 7. Mesh of the test sandwich plate.

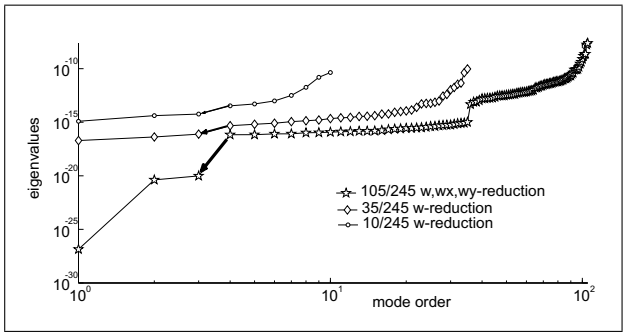

Figure 8. Spectrum of a2-Laurent coefficient at various stages of reduction of the undamped sandwich plate.

Table II. Material properties of the test sandwich plate. Young's modulus E, Poisson's ratio ν, Density ρ and Loss factor η.

Elastic layers	Viscoelastic core
$E_{1,2} = 7 \cdot 10^{10}\,\mathrm{N/m^2}$	$E_0 = 5.2 \cdot 10^6\,\mathrm{N/m^2}$
$\nu_{1,2} = 0.33$	$\nu_0 = 0.3$
$\rho_{1,2} = 2720\,\mathrm{kg/m^3}$	$\rho_0 = 1015\,\mathrm{kg/m^3}$
$\eta_{1,2} = 0$	$\eta_0 = 1$

and fourth eigenvalues, which means that the reduced dimension $\hat{\sigma}$ (which has been introduced in §4.3.2 to characterize stress-free motions observable in the reduced coordinates) takes presently the value $\hat{\sigma} = 3$. This value precisely corresponds to the maximum that can be detected on a set of a vertical direction and two rotations. However, there are $\sigma = 6$ independent stress-free motions in the initial model before condensation. There are thus $\sigma - \hat{\sigma} = 3$ motions satisfying $\boldsymbol{K}_s = 0$ and are zero in the condensation set. Writing for each of these displacements

$$\begin{bmatrix} \boldsymbol{K}_{aa} & \boldsymbol{K}_{ad} \\ \boldsymbol{K}_{da} & \boldsymbol{K}_{dd} \end{bmatrix} \begin{pmatrix} \boldsymbol{0} \\ \boldsymbol{s}_d \end{pmatrix} = \boldsymbol{0} \quad \Rightarrow \quad \boldsymbol{K}_{dd}\boldsymbol{s}_d = \boldsymbol{0} \qquad (57)$$

gives the conclusion that block $\boldsymbol{K}_{dd}$ being not invertible, Guyan formulae are totally inappropriate to solve this reduction problem.

Figure 9 shows the series of progressively converging receptance functions calculated in the z-direction at location 4 of the plate before introducing damping (except a numerical conventional structural damping of 0.1%).

Figure 10 illustrates what can be expected when uncensored raw coefficients are introduced in the retrieval

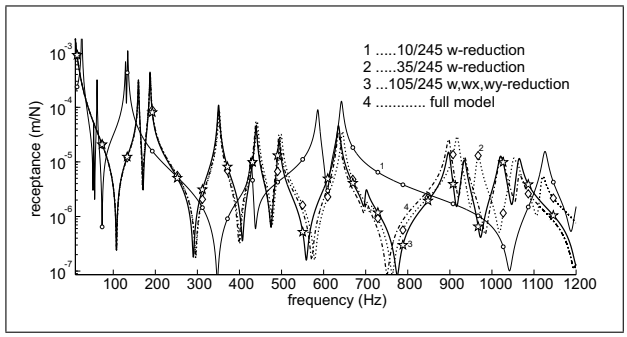

Figure 9. Receptance at plate location 4-z at various stages of reduction of the undamped sandwich plate.

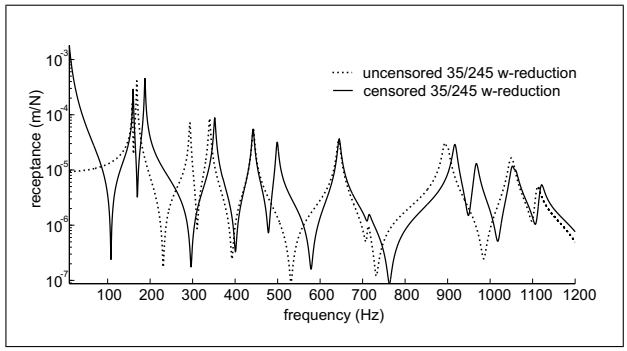

Figure 10. Influence of censoring.

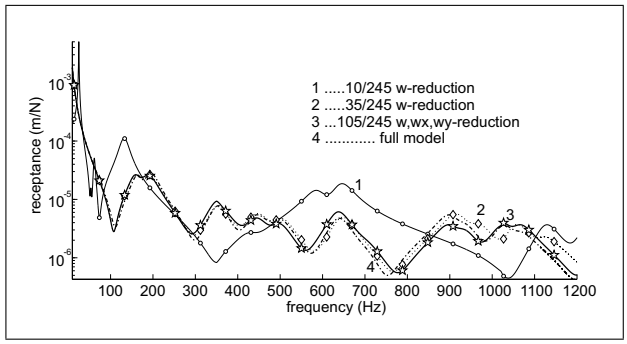

Figure 11. Receptance at plate location 4-z at various stages of reduction of the damped sandwich plate.

formulae. Considering the extremely low numerical levels which can be observed in Figure 8, it is important to say that setting to zero an eigenvalue $\lambda = 10^{-20}$ is not expected to modify the Laurent coefficient itself, but is just as putting a stamp on the eigenvalue so that the corresponding eigenvector will be recognized by the computer program as a null vector to be integrated in the kernel. In other words, the operation has no sense if the raw coefficient is not very close to singularity, and does not present a neat gap in its series of eigenvalues. The 10/245 reduced FRF in Figure 9 is a good example of what happens when one tries to jump over this barrier.

Figure 11 shows the series of receptance functions obtained, as in the previous case, in the z-direction at location 4 of the plate after reintroducing realistic damping characteristics by the MSE method.

6. Vibro-acoustic test examples

Important developments are still required for the explicit reduction method to become an industrial one dealing with models of growing size and complexity, especially concerning the control on numerical zeros, which is a critical point in censoring operations, and the development of efficient algorithms. To encourage the corresponding developments, it has been judged worthwhile to include reduced models as soon as possible, at the present stage of development, in more realistic acoustic simulations than the mere computation of structural transfer functions. The test examples that will now be presented are reconstitutions of experimental results taken from the literature, through independent numerical modeling based on the geometric and material properties given by their authors and involving, at some step, the condensation technique of the preceding sections.

6.1. Vibro-acoustic formulation

Two papers with experimental data have been taken as references:

- The first example, studied by Foin *et al.* [24], deals with the computation and measurement of the mean square velocity of a baffled sandwich plate excited by a point force and immersed in air;
- The second example, studied by Lee *et al.* [25], deals with the computation and measurement of the transmission loss factors (TL) of three geometric configurations of a simply supported sandwich plate excited by a diffuse sound field.

For both examples, the vibro-acoustic model consists of a sandwich plate mounted in a rigid, infinite plane baffle separating two semi-infinite fluid domains: the excitation domain and the receiver domain. The plate is assumed to be subjected to mechanical or acoustic excitations. The corresponding coupled structural-acoustic equation of motion is given by [20]

$$\left[\hat{\boldsymbol{k}}(\omega) - \omega^2\left(\boldsymbol{m} + \boldsymbol{Z}_R(\omega)\right)\right]\boldsymbol{u}(\omega) = \boldsymbol{F}_a(\omega) + \boldsymbol{F}_m(\omega), \quad (58)$$

where $\hat{\boldsymbol{k}}$ and $\boldsymbol{m}$ are the condensed stiffness and mass matrices of the sandwich plate, $\boldsymbol{Z}_R$ is the radiation impedance matrix of the fluid, and $\boldsymbol{F}_a$ and $\boldsymbol{F}_m$ are the force vectors due to the acoustic and mechanical excitations, respectively. In this study, the numerical computation of $\boldsymbol{Z}_R$ is performed using a boundary element method [32]. A reduction to the classical three dofs per node for bending plates: w, $w_{,x}$ and $w_{,y}$ has been retained here.

6.2. Foin example

Foin *et al.* [24] studied the vibration response of a baffled, simply supported base plate fully covered with constrained damping treatment and excited by a point source. The plate is 0.48 m long and 0.42 m wide. The elastic faces are made from aluminum. The base plate is 3 mm thick and the constraining layer is 0.5 mm thick. The viscoelastic core (ISD 112 manufactured by 3M) is 0.25 mm thick. The material properties of the aluminum and the ISD 112 are given in Table III. The mean square velocity of the plate immersed in air was measured by Foin *et al.* in the 50–800 Hz frequency range. The plate was driven by a shaker at coordinates x=0.07 m, y=0.08 m from a corner of the plate. The vibration velocity of the plate was measured with a laser vibrometer. The vibration response of the base plate alone was also measured. In the present study, the sandwich plate is modeled by 720 triangular elements (18×20×2) and 399 nodes. The initial model before reduction thus contains 2793 dofs. The computation of the mean square velocity is performed in the frequency band of 50–800 Hz with a step of 1 Hz. The reduction to three dofs per node leads to a model of 1197 dofs. In order to evaluate the gain of the presented method in terms of computing time, a comparison of the computational time for the initial model and the reduced model is first performed. The computations are carried out using an Intel Xeon 3GHz CPU, 16GB RAM machine. The comparison shows that the computation for the reduced model is 5.4 times faster than for the initial model due to the reduced size of the stiffness and mass matrices (298 s vs. 1611 s). If we include the time needed for the condensation step (298 s) then the overall computational time for the reduced model is 3.3 times faster. In this comparison, the computational time of the radiation impedance matrix is not included. As has been shown in [24], its variation with respect to frequency is smooth. Thus, a frequency interpolation technique is used to evaluate its components. This technique consists in first computing at master frequencies with a given step (for instance, a step of 100 Hz has been adopted in this example) and then interpolating its value at the current frequency when solving the vibro-acoustic equation of motion (58). This method is very useful to decrease the computational time without decreasing the accuracy of the results.

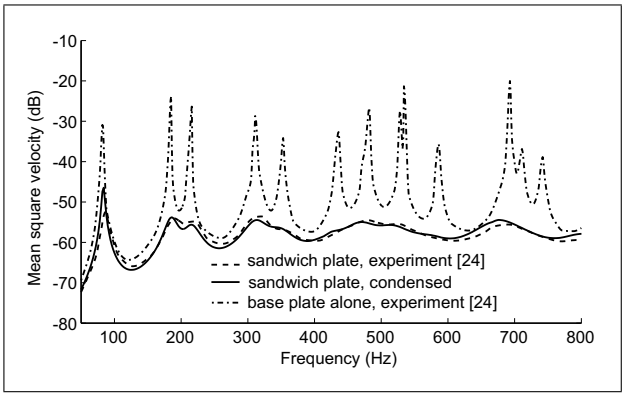

Figure 12. Mean square velocity of a base plate alone and then fully covered with constrained damping treatment. Comparison between the results calculated from the condensed model and the experimental results reported by Foin *et al.* [24].

Figure 12 presents the mean square velocity of the sandwich plate against the frequency predicted by the condensed model and compared with the experimental results reported by Foin *et al.* Good agreement is observed between these results. For comparison, the mean square ve-

Table III. Material properties of the 3M-ISD 112 sandwich plate. Young's modulus E, Poisson's ratio ν, Density ρ and Loss factor η.

Elastic layers	Viscoelastic core
$E_{1,2} = 6.6 \cdot 10^{10}\,\mathrm{N/m^2}$	$E_0 = 5.2 \cdot 10^{6}\,\mathrm{N/m^2}$
$\nu_{1,2} = 0.33$	$\nu_0 = 0.3$
$\rho_{1,2} = 2680\,\mathrm{kg/m^3}$	$\rho_0 = 1015\,\mathrm{kg/m^3}$
$\eta_{1,2} = 0$	$\eta_0 = 1$ at 25 °C, 500 Hz

Table IV. Test sample thicknesses (mm).

Sample	Face 1 (h_1)	Core (h_0)	Face 2 (h_2)
S1 (symmetric)	0.5	1	0.5
S2 (symmetric)	0.5	2	0.5
S3 (asymmetric)	0.5	1	1

Table V. Material properties of the test samples. Young's modulus E, Poisson's ratio ν, Density ρ and Loss factor η.

Elastic layers	Viscoelastic core
$E_{1,2} = 7.32 \cdot 10^{10}\,\mathrm{N/m^2}$	$E_0 = 2.67 \cdot 10^{6}\,\mathrm{N/m^2}$
$\nu_{1,2} = 0.33$	$\nu_0 = 0.4$
$\rho_{1,2} = 2720\,\mathrm{kg/m^3}$	$\rho_0 = 1600\,\mathrm{kg/m^3}$
$\eta_{1,2} = 0$	$\eta_0 = 0.7$ at 15 °C, 500 Hz

locity of the base plate alone is also presented. Compared to the base plate response, it can be seen that the sandwich plate response is very damped, mainly at the resonance frequencies.

6.3. Lee example

Lee *et al.* [25] studied experimentally the TL of three configurations of a simply supported sandwich plate. To measure the noise TL characteristics, they placed the experimental samples between two reverberation chambers with the same dimensions: 0.5 m×0.6 m×0.7 m. In the source chamber, a diffuse sound field was provided by a speaker source. The receiving chamber was acoustically and structurally isolated from the source chamber. Sound was transmitted to the receiving chamber only by way of the simply supported test panel. The transmission loss of the test sample was then calculated from the difference between the averages of the sound pressure levels, measured in each of the chambers by a microphone, and corrected by the sound absorption of the receiving chamber. In the following, the results of three rectangular test samples are presented; two are symmetric (S1 and S2) and one is asymmetric (S3). Their dimensions are 0.303 m×0.203 m. The thicknesses and material properties are listed in Tables IV and V, respectively. The core is a viscoelastic high damping polymer material made by the Kurashiki Chemical Co. [25].

Figures 13–15 compare the calculated diffuse sound TL from the present condensation model with the experimental results obtained by Lee *et al.* for the symmetric (S1,S2) and asymmetric (S3) configurations. The curves

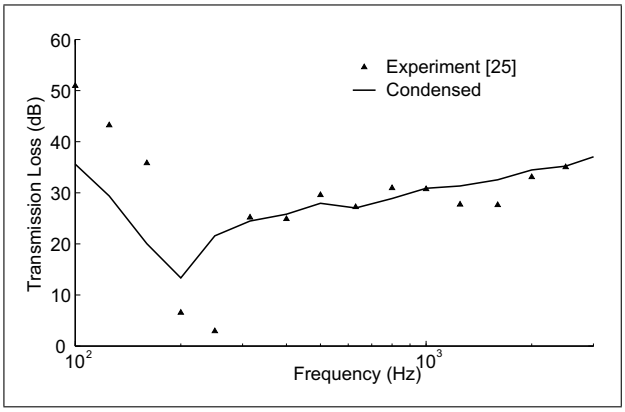

Figure 13. Comparison between the TL calculated from the condensed model and the experimental results obtained by Lee *et al.* [25]. Symmetric configuration S1.

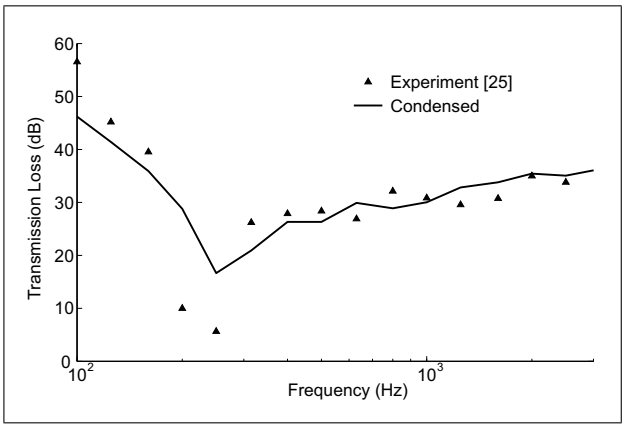

Figure 14. Comparison between the TL calculated from the condensed model and the experimental results obtained by Lee *et al.* [25]. Symmetric configuration S2.

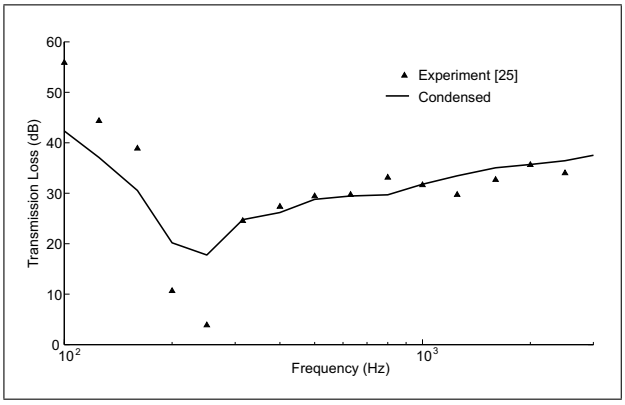

Figure 15. Comparison between the TL calculated from the condensed model and the experimental results obtained by Lee *et al.* [25]. Asymmetric configuration S3.

are presented in third-octave bands in the frequency range [100–3000] Hz. The agreement between the TL curves calculated by the present formulation and the experimental curves is very good. In the low frequency range, the drops in the measured TL values are due to the resonances of the chambers used in the experimental set-up, which means

that the condition of the diffuse field sound is insufficient at low frequencies [25]. It can also be seen that, in the three configurations, the first mode of the plates produces a large resonant dip in the transmission loss. It should be noted that, due to the small size of the rooms used in the acoustic test set-up, the conditions of the diffuse sound field are not sufficient in the low frequency range. Lee *et al.* did not give the sound absorption coefficient they measured for the rooms to estimate the Schroeder frequency, but Figures 13–15 show clearly the drops in the measured TL values due to the resonance frequencies of the rooms.

7. Conclusion

An interesting approach to the model reduction problem has been developed, which is mainly based on the analysis of singularity in free-floating systems. The proposed method opens up Guyan reduction, which is here naturally integrated into complete families of modal reductions. It has been shown that the studied examples introduce a class of reductions in physical coordinates which cannot be performed using the Guyan technique. Finally, promising examples of effective reductions of sandwich structures have been carried out, which provide the proof that reasonable models of sandwich structures and damping properties, used with adequate explicit reductions, enable the reconstitution of the results found in the literature on an ordinary laptop computer. However, to improve the efficiency of the proposed approach, the following points need to be addressed:

- A better detection of singularity than the rapid "inspection" proposed in this paper is clearly required;
- Effective estimations of errors remain to be carried out;
- Mastering generalized coordinates, which is the key to large structural sizes, is still at an early stage.

Finally, bridging the gap between P-matrices of explicit methods and Ritz-Galerkin T-matrices would be of considerable interest, since this could lead to new approaches where the discussion and choice of variables could be carried out through explicit analysis and the effective numerical reduction through improved Ritz-Galerkin techniques.

Appendix

A1. Pseudo-inversion of rectangular systems of maximum rank

A1.1. Aims and scope

This appendix is devoted to auxiliary rectangular systems of the form

$$\boldsymbol{S}\boldsymbol{x} = \boldsymbol{f}, \tag{A1}$$

with $\boldsymbol{S}$ a rectangular (p, q)-matrix, $p \neq q$; $\boldsymbol{x}$ the q-vector of unknowns and $\boldsymbol{f}$ a given p-vector. It is important to recall how least squares techniques can be used either to deliver approximate pseudo-solutions in the case of overdetermination, $p > q$, or to make a choice from an infinity of solutions in the case of underdetermination, $p < q$.

A1.2. The maximum rank condition

To avoid unnecessary complications, it will be assumed that matrix $\boldsymbol{S}$ satisfies the maximum rank condition

$$\operatorname{rank}(\boldsymbol{S}) = \min(p, q). \tag{A2}$$

In other words, matrix $\boldsymbol{S}$ is constituted either by q independent p-columns when $p > q$ or by p independent q-rows when $q < p$. The whole interest of this lies in the fact that

$$\det(\boldsymbol{S}^T\boldsymbol{S}) \neq 0 \quad \text{if} p > q, \tag{A3}$$

$$\det(\boldsymbol{S}\boldsymbol{S}^T) \neq 0 \quad \text{if} p < q. \tag{A4}$$

A1.3. Lagrange lemma

An important lemma, which is indeed the very basis of duality and Lagrange multipliers theory, stipulates that for an arbitrary rectangular or square matrix $\boldsymbol{S}$

$$\left(\ker\boldsymbol{S}\right)^{\perp} = \operatorname{range}(\boldsymbol{S}^T) \tag{A5}$$

which indeed is another way to say that $\langle \boldsymbol{x}, \boldsymbol{S}\boldsymbol{y}\rangle = \langle \boldsymbol{S}^T\boldsymbol{x}, \boldsymbol{y}\rangle$.

A1.4. Pseudo-inversion of rectangular overdetermined systems

There is no solution to the inversion problem but it remains possible to replace the solution of (A1) by the minimization of the distance from $\boldsymbol{S}\boldsymbol{x}$ to $\boldsymbol{f}$:

find x^* that minimizes

$$F(\boldsymbol{x}) = \frac{1}{2}||\boldsymbol{S}\boldsymbol{x} - \boldsymbol{f}||^2. \tag{A6}$$

For the usual Euclidian norm and scalar product, $\langle\ \rangle$, function F and its first variation δF, can be written as

$$\begin{aligned} F(\boldsymbol{x}) &= \frac{1}{2}\boldsymbol{x}^T\boldsymbol{S}^T\boldsymbol{S}\boldsymbol{x} - \frac{1}{2}\left(\boldsymbol{x}^T\boldsymbol{S}^T\boldsymbol{f} + \boldsymbol{f}^T\boldsymbol{S}\boldsymbol{x}\right) + \frac{1}{2}\boldsymbol{f}^T\boldsymbol{f} \\ &= \frac{1}{2}\left\langle \boldsymbol{S}^T\boldsymbol{S}\boldsymbol{x}\,\middle|\,\boldsymbol{x}\right\rangle - \left\langle \boldsymbol{S}^T\boldsymbol{f}\,\middle|\,\boldsymbol{x}\right\rangle + \frac{1}{2}\boldsymbol{f}^T\boldsymbol{f}, \end{aligned} \tag{A7}$$

$$\begin{aligned} \delta F(\boldsymbol{x}) &= \frac{1}{2}\left\langle \boldsymbol{S}^T\boldsymbol{S}\delta\boldsymbol{x}\,\middle|\,\boldsymbol{x}\right\rangle + \frac{1}{2}\left\langle \boldsymbol{S}^T\boldsymbol{S}\boldsymbol{x}\,\middle|\,\delta\boldsymbol{x}\right\rangle \\ &\quad - \left\langle \boldsymbol{S}^T\boldsymbol{f}\,\middle|\,\delta\boldsymbol{x}\right\rangle \\ &= \left\langle \boldsymbol{S}^T\boldsymbol{S}\boldsymbol{x} - \boldsymbol{S}^T\boldsymbol{f}\,\middle|\,\delta\boldsymbol{x}\right\rangle. \end{aligned} \tag{A8}$$

Matrix $\boldsymbol{S}^T\boldsymbol{S}$ is invertible by (A3). The stationarity condition, $\delta F(\boldsymbol{x}) = 0$, $\forall\delta\boldsymbol{x}$, thus brings out

$$\boldsymbol{x}^* = (\boldsymbol{S}^T\boldsymbol{S})^{-1}\boldsymbol{S}^T\boldsymbol{f}. \tag{A9}$$

The ordinary Euclidian metrics can be replaced by any M-distance, based on a positive definite symmetric matrix $\boldsymbol{M}$. This leads to

$$\begin{aligned} G(\boldsymbol{x}) &= \frac{1}{2}\left(\boldsymbol{S}\boldsymbol{x} - \boldsymbol{f}\right)^T\boldsymbol{M}\left(\boldsymbol{S}\boldsymbol{x} - \boldsymbol{f}\right) \\ &= \frac{1}{2}\left\langle \boldsymbol{S}^T\boldsymbol{M}\boldsymbol{S}\boldsymbol{x}\,\middle|\,\boldsymbol{x}\right\rangle - \left\langle \boldsymbol{S}^T\boldsymbol{M}\boldsymbol{f}\,\middle|\,\boldsymbol{x}\right\rangle \\ &\quad + \frac{1}{2}\boldsymbol{f}^T\boldsymbol{M}\boldsymbol{f}, \end{aligned} \tag{A10}$$

$$\delta G(\boldsymbol{x}) = \left\langle \boldsymbol{S}^T\boldsymbol{M}\boldsymbol{S}\boldsymbol{x} - \boldsymbol{S}^T\boldsymbol{M}\boldsymbol{f}\,\middle|\,\delta\boldsymbol{x}\right\rangle. \tag{A11}$$

The M-pseudo-inverse is then found as

$$\boldsymbol{x}_M = \left(\boldsymbol{S}^T\boldsymbol{M}\boldsymbol{S}\right)^{-1}\boldsymbol{S}^T\boldsymbol{M}\boldsymbol{f}. \tag{A12}$$

A1.5. Pseudo-inversion of rectangular underdetermined systems

The number p of equations is now smaller than the number q of unknowns. By the maximum rank hypothesis, the p equations are linearly independent and system (A1) admits an infinite set of solutions. Distinguished solutions can however be isolated by minimizing the distance to $\boldsymbol{f}$.

A1.5.1. Minimization of Euclidian distance

Find x^* that minimizes

$$H(\boldsymbol{x}) = \frac{1}{2}||\boldsymbol{x}||^2, \tag{A13}$$

subject to $\boldsymbol{S}\boldsymbol{x} = \boldsymbol{f}$.

Function H and the first variation δH are written

$$H(\boldsymbol{x}) = \frac{1}{2}\boldsymbol{x}^T\boldsymbol{x}, \tag{A14}$$

$$\delta H(\boldsymbol{x}) = \boldsymbol{x}^T\delta\boldsymbol{x} = \left\langle \boldsymbol{x} \,\middle|\, \delta\boldsymbol{x} \right\rangle. \tag{A15}$$

At the optimum, the first variation, $\delta H(\boldsymbol{x}^*) = \langle \boldsymbol{x}^*, \delta\boldsymbol{x}\rangle$ must remain insensitive to any admissible $\delta\boldsymbol{x}$, such that $\boldsymbol{S}\delta\boldsymbol{x} = 0$ or, in other words, such that $\delta\boldsymbol{x} \in \ker\boldsymbol{S}$. Thus, the condition of stationarity is that any $\delta\boldsymbol{x}$ in $\ker\boldsymbol{S}$ is orthogonal to $\boldsymbol{x}^*$. By the Lagrange lemma

$$\boldsymbol{x}^* \in \left(\ker\boldsymbol{S}\right)^\perp = \mathrm{range}(\boldsymbol{S}^T) \tag{A16}$$

and there is some vector of Lagrange multipliers $\Lambda \in R^p$, such that

$$\boldsymbol{x}^* = \boldsymbol{S}^T\boldsymbol{\Lambda}. \tag{A17}$$

Substituting for $\boldsymbol{x} = \boldsymbol{x}^*$ in equation (A1), the expression given by equation (A17) yields

$$\boldsymbol{S}\boldsymbol{S}^T\boldsymbol{\Lambda} = \boldsymbol{f}. \tag{A18}$$

Because $\boldsymbol{S}\boldsymbol{S}^T$ is invertible by (A4), this fully determines the Lagrange multipliers

$$\boldsymbol{x}^* = \boldsymbol{S}^T\left(\boldsymbol{S}^T\boldsymbol{S}\right)^{-1}\boldsymbol{f}. \tag{A19}$$

A1.5.2. Minimization of an arbitrary M-distance

Any metric, based on a symmetric positive definite matrix $\boldsymbol{M}$, can be substituted for the ordinary Euclidian metric to reformulate the minimization problem as

Find $\boldsymbol{x}_M$ that minimizes

$$J(\boldsymbol{x}) = \frac{1}{2}||\boldsymbol{x}||_M^2 = \frac{1}{2}\boldsymbol{x}^T\boldsymbol{M}\boldsymbol{x}, \tag{A20}$$

subject to $\boldsymbol{S}\boldsymbol{x} = \boldsymbol{f}$.

The first variation is now written

$$\delta J(\boldsymbol{x}) = \boldsymbol{x}^T\boldsymbol{M}\delta\boldsymbol{x} + \delta\boldsymbol{x}^T\boldsymbol{M}\boldsymbol{x} = \left\langle \boldsymbol{M}\boldsymbol{x} \,\middle|\, \delta\boldsymbol{x} \right\rangle. \tag{A21}$$

Stationarity at $\boldsymbol{x}_M$ imposes

$$\boldsymbol{M}\boldsymbol{x}_M \in (\ker\boldsymbol{S})^\perp = \mathrm{range}(\boldsymbol{S}^T).$$

There is then no difficulty in writing the optimum as

$$\boldsymbol{x}_M = \boldsymbol{M}^{-1}\boldsymbol{S}^T\left(\boldsymbol{S}\boldsymbol{M}^{-1}\boldsymbol{S}^T\right)^{-1}\boldsymbol{f}. \tag{A22}$$

A1.5.3. Expression of projectors

Equations (A9) and (A12) deserve special attention in the context of Structural Dynamics applications where $\boldsymbol{S}$ will be the spanning matrix of the set of rigid body motions and $\boldsymbol{M}$ the mass matrix. Equation (A9) defines $\boldsymbol{x}^*$ such that $\boldsymbol{S}\boldsymbol{x}^*$ is the vector of range$\boldsymbol{S}$ that lies at the shortest distance from the given $\boldsymbol{f}$. The orthogonal projector on the subspace generated by the columns of $\boldsymbol{S}$, is thus given by

$$\boldsymbol{\Pi} = \boldsymbol{S}\left(\boldsymbol{S}^T\boldsymbol{S}\right)^{-1}\boldsymbol{S}^T. \tag{A23}$$

Similarly, equation (A12) defines the M-projector as

$$\boldsymbol{\Pi}_M = \boldsymbol{S}\left(\boldsymbol{S}^T\boldsymbol{M}\boldsymbol{S}\right)^{-1}\boldsymbol{S}^T\boldsymbol{M}. \tag{A24}$$

A2. Pseudo-inversion of square symmetric singular matrices

A2.1. Aims and scope

The present section is devoted to quite useful, although unusual, projector representations of pseudo-inverses of square symmetric singular systems in the form

$$\boldsymbol{K}\boldsymbol{x} = \boldsymbol{f}. \tag{A25}$$

It is supposed that the kernel of $\boldsymbol{K}$ is characterized by a spanning matrix $\boldsymbol{S}$ such that

$$\begin{aligned}\ker(\boldsymbol{K}) &= \mathrm{range}(\boldsymbol{S}) \\ &= \left\{\boldsymbol{y} \in R^p \,\middle|\, \exists\boldsymbol{\beta} \in R^q : \boldsymbol{y} = \boldsymbol{S}\boldsymbol{\beta}\right\}.\end{aligned} \tag{A26}$$

Although the presentation is quite general, $\boldsymbol{K}$ can be viewed as a stiffness matrix and $\boldsymbol{S}$ as related to the corresponding set of rigid body motions or mechanisms.

A2.2. Lagrange lemma for symmetric matrices

For any symmetric matrix $\boldsymbol{K}$, the Lagrange lemma (A5) takes the form

$$\left(\ker\boldsymbol{K}\right)^\perp = \mathrm{range}(\boldsymbol{K}). \tag{A27}$$

A2.3. Integrability condition and set of solutions

System (A25) has at least one solution $\boldsymbol{x}_0$ if $\boldsymbol{f}$ lies in the range of $\boldsymbol{K}$, or, by Lagrange's lemma, is orthogonal to $((S))$, i.e. if it satisfies the so-called "integrability condition"

$$\boldsymbol{S}^T\boldsymbol{f} = 0. \tag{A28}$$

In this case, the complete set of solutions can be expressed, in terms of an arbitrary $\boldsymbol{\alpha}$, by

$$\boldsymbol{x} = \boldsymbol{x}_0 + \boldsymbol{S}\boldsymbol{\alpha}. \tag{A29}$$

The point is to produce additional conditions or relations that constrain the initial system to deliver a well-posed problem and a well-defined $\boldsymbol{x}_0$.

A2.4. Moore-Penrose or SVD pseudo-inverse

Projector theorem. *Provided* $\boldsymbol{f}$ *satisfies the integrability condition* $\boldsymbol{S}^T\boldsymbol{f} = \boldsymbol{0}$,

$$\left\{ \begin{array}{c} \boldsymbol{K}\boldsymbol{x} = \boldsymbol{f} \\ \boldsymbol{S}^T\boldsymbol{x} = \boldsymbol{0} \end{array} \right\} \quad \Longleftrightarrow \qquad \text{(A30)}$$

$$\boldsymbol{x} = \boldsymbol{x}_0 = \left(\lambda\boldsymbol{\Pi} + \boldsymbol{K}\right)^{-1}\boldsymbol{f}, \quad \forall\lambda \neq 0,$$

where λ *is an arbitrary non-zero number and* $\boldsymbol{\Pi}$ *is the orthogonal projector onto* $\ker\boldsymbol{K}$.

The solution can be identified as the only element of $\text{range}\boldsymbol{K}$ *that satisfies* $\boldsymbol{K}\boldsymbol{x} = \boldsymbol{f}$ *or, in other words, is the SVD pseudo-inverse of the symmetric matrix* $\boldsymbol{K}$.

Proof. For each $\lambda \neq 0$, $\lambda\boldsymbol{\Pi} + \boldsymbol{K}$ is invertible. Indeed, assuming $(\lambda\boldsymbol{\Pi} + \boldsymbol{K})\boldsymbol{x} = 0$ brings a decomposition of zero -$\lambda\boldsymbol{\Pi}\boldsymbol{x} + \boldsymbol{K}\boldsymbol{x}$- on a pair -$\ker\boldsymbol{K}$, $\text{range}\boldsymbol{K}$- of mutually orthogonal subspaces. Each term of the decomposition is necessarily equal to zero, and it comes out that $\lambda\boldsymbol{\Pi}\boldsymbol{x} = 0$ and $\boldsymbol{K}\boldsymbol{x} = 0$. Because $\lambda \neq 0$, the left-hand equation shows that $\boldsymbol{\Pi}\boldsymbol{x} = 0$ and therefore that $\boldsymbol{x}$ is an element of $\text{range}\boldsymbol{K}$, while the right-hand shows that it should simultaneously belong to the orthogonal complement $\ker(\boldsymbol{K})$. In other words, $\boldsymbol{x}$ is necessarily the zero-vector and $(\lambda\boldsymbol{\Pi} + \boldsymbol{K})$ is invertible.

From this, for every $\boldsymbol{f}$, satisfying the integrability condition $\boldsymbol{S}^T\boldsymbol{f} = 0$, there are some $\boldsymbol{x}^*$ such that $\boldsymbol{x}^* = (\lambda\boldsymbol{\Pi} + \boldsymbol{K})^{-1}\boldsymbol{f}$. When $\boldsymbol{f}$ satisfies the integrability condition, $\lambda\boldsymbol{\Pi}\boldsymbol{x}^* + (\boldsymbol{K}\boldsymbol{x}^* - \boldsymbol{f}) = 0$ is again a decomposition of zero on the two orthogonal complementary subspaces, $\ker\boldsymbol{K}$, $\text{range}\boldsymbol{K}$. The conclusion, with $\lambda \neq 0$, is that $\boldsymbol{x}^*$ satisfies $\boldsymbol{\Pi}\boldsymbol{x}^* = 0$ and $\boldsymbol{K}\boldsymbol{x}^* - \boldsymbol{f} = 0$. The former condition means that $\boldsymbol{x}^*$ lies in $\text{range}\boldsymbol{K}$, and the latter is the solution to $\boldsymbol{K}\boldsymbol{x} = \boldsymbol{f}$. It is in fact the only element of $\text{range}\boldsymbol{K}$ to have this property, since two such elements -$\boldsymbol{x}_1, \boldsymbol{x}_2$- should satisfy $\boldsymbol{x}_1 - \boldsymbol{x}_2 \in \text{range}\boldsymbol{K}$ and, at the same time, $\boldsymbol{x}_1 - \boldsymbol{x}_2 \in \ker\boldsymbol{K}$. Solution $\boldsymbol{x}^*$ is referred to as "SVD pseudo-inverse" of $\boldsymbol{K}$.

An important remark is that, as long as $\boldsymbol{f}$ strictly obeys the integrability condition and λ is not zero, $\boldsymbol{x}^*$ is totally independent of λ, which surprisingly plays the role of a "joker". When $\boldsymbol{K}$ is a stiffness matrix, $(\lambda\boldsymbol{\Pi} + \boldsymbol{K})^{-1}$ can be considered as an extension of the associated intrinsic flexibility, which coincides with this flexibility when applied to an admissible self-equilibrated system of loads and otherwise depends on λ.

A2.5. Inertia-relief pseudo-inverse

M-projector theorem. *Provided* $\boldsymbol{f}$ *satisfies the integrability condition* $\boldsymbol{S}^T\boldsymbol{f} = \boldsymbol{0}$,

$$\left\{ \begin{array}{c} \boldsymbol{K}\boldsymbol{x} = \boldsymbol{f} \\ \boldsymbol{S}^T\boldsymbol{M}\boldsymbol{x} = \boldsymbol{0} \end{array} \right\} \quad \Longleftrightarrow \qquad \text{(A31)}$$

$$\boldsymbol{x} = \boldsymbol{x}_M = \left(1 - \boldsymbol{\Pi}_M\right)\left(\lambda\boldsymbol{\Pi} + \boldsymbol{K}\right)^{-1}\boldsymbol{f}, \quad \forall\lambda \neq 0,$$

where $\boldsymbol{\Pi}$, λ *are defined as above, and where* $\boldsymbol{\Pi}_M$ *is the M-projector onto* $\ker\boldsymbol{K}$.

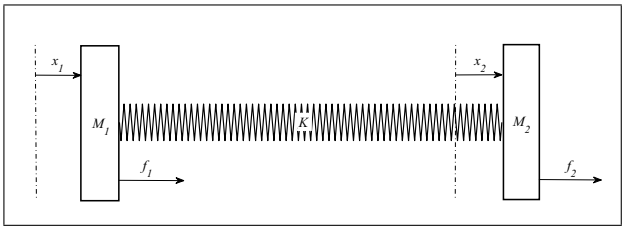

Figure A1. Illustrative example of a 1D system consisting of two masses and a spring.

Proof. Using (A29) with the special solution $\boldsymbol{x}_0 = \boldsymbol{x}^*$, given by (A30), one can write

$$\boldsymbol{x}_M = \left(\lambda\boldsymbol{\Pi} + \boldsymbol{K}\right)^{-1}\boldsymbol{f} + \boldsymbol{S}\boldsymbol{\alpha}, \qquad \text{(A32)}$$

and then determine the unknown vector, $\boldsymbol{\alpha}$, by the orthogonality condition $\boldsymbol{S}^T\boldsymbol{M}\boldsymbol{x}^m = \boldsymbol{0}$. It is easily found after a few computations that

$$\boldsymbol{x}_M = \left[1 - \boldsymbol{S}\left(\boldsymbol{S}^T\boldsymbol{M}\boldsymbol{S}\right)^{-1}\boldsymbol{S}^T\boldsymbol{M}\right]\left(\lambda\boldsymbol{\Pi} + \boldsymbol{K}\right)^{-1}\boldsymbol{f}. \qquad \text{(A33)}$$

Expression (A24) of the M-projector then brings the conclusion.

A2.6. Application to Structural Dynamics

All formulae of this Appendix are intended to be directly applied to Structural Mechanics problems. In this context, $\boldsymbol{M}$ effectively denotes a mass matrix, while $\boldsymbol{K}$ is a singular stiffness matrix, associated with a matrix $\boldsymbol{S}$, of mechanisms or rigid-body motions. Table A1 illustrates the mechanical signification of algebraic formulae, concerning especially the $\boldsymbol{\Pi}$-projector for the example of a 1D free-floating system consisting of two masses M_1 and M_2 and connected by a spring of stiffness K as shown in Figure A1.

A3. Laurent expansion of dynamic responses and receptances

A3.1. Introduction

The Taylor formulae for fixed systems have been developed in section 3. The present appendix only addresses the singular case of a free-floating system. It should be recalled that matrix $\boldsymbol{K}$ is in this case a $N \times N$ singular matrix of rank $N - \sigma$, and that it is convenient to denote $\boldsymbol{S}$ a $N \times \sigma$ spanning matrix of $\ker\boldsymbol{K}$. To facilitate the introduction and discussion of inertial and inertia relief terms, which are of special interest in Structural Dynamics, it has been thought wiser to present the elementary expansion of the dynamical response to a given excitation before extracting the matrix coefficients.

The dynamic response, $\boldsymbol{x}$, to an excitation $\boldsymbol{f}$, is solution to the basic equation of motion

$$\left(\boldsymbol{K} - \boldsymbol{M}\omega^2\right)\boldsymbol{x} = \boldsymbol{f}. \qquad \text{(A34)}$$

Table A1. **Π**-projector formulae for the 2-mass 1D system of Figure A1.

1. Mass and stiffness matrices : $\mathbf{M}=\begin{bmatrix} M_1 & 0 \\ 0 & M_2 \end{bmatrix}$; $\mathbf{K}=\begin{bmatrix} K & -K \\ -K & K \end{bmatrix}$

2. Rigid body motions : $ker\,\mathbf{K}=((\mathbf{S}))\ \ with\ \ \mathbf{S}=\begin{pmatrix}1\\1\end{pmatrix}$; $\sigma = dim\,(ker\,\mathbf{K})=1$

3. Self-equilibrated systems of forces:

$$range\,\mathbf{K}=(ker\,\mathbf{K})^{\perp}=\{\mathbf{f}:\mathbf{S}^{\mathrm{T}}\mathbf{f}=\mathbf{0}\}=\{\mathbf{f}:\ f_1+f_2=0\}$$

4. Orthogonal projector to $ker\,\mathbf{K}$:

$$(\mathbf{S}^{\mathrm{T}}\mathbf{S})^{-1}\mathbf{S}^{\mathrm{T}}=\left[\begin{pmatrix}1 & 1\end{pmatrix}\begin{pmatrix}1\\1\end{pmatrix}\right]^{-1}\begin{pmatrix}1 & 1\end{pmatrix}=\begin{pmatrix}\frac{1}{2} & \frac{1}{2}\end{pmatrix},\ \boldsymbol{\Pi}=\mathbf{S}(\mathbf{S}^{\mathrm{T}}\mathbf{S})^{-1}\mathbf{S}^{\mathrm{T}}=\begin{pmatrix}1\\1\end{pmatrix}\begin{pmatrix}\frac{1}{2} & \frac{1}{2}\end{pmatrix}=\begin{bmatrix}\frac{1}{2} & \frac{1}{2}\\ \frac{1}{2} & \frac{1}{2}\end{bmatrix}$$

5. SVD pseudo-inverse of $\mathbf{K}$:

$$(\lambda\boldsymbol{\Pi}+\mathbf{K})^{-1}=\begin{bmatrix}\frac{\lambda}{2}+K & \frac{\lambda}{2}-K\\ \frac{\lambda}{2}-K & \frac{\lambda}{2}+K\end{bmatrix}^{-1}=\frac{1}{\left(\frac{\lambda}{2}+K\right)^2-\left(\frac{\lambda}{2}-K\right)^2}\begin{bmatrix}K+\frac{\lambda}{2} & K-\frac{\lambda}{2}\\ K-\frac{\lambda}{2} & K+\frac{\lambda}{2}\end{bmatrix}$$

$$=\frac{1}{2\lambda K}\begin{bmatrix}K+\frac{\lambda}{2} & K-\frac{\lambda}{2}\\ K-\frac{\lambda}{2} & K+\frac{\lambda}{2}\end{bmatrix}$$

- Independence of λ under self-equilibrated systems of forces:

$$(\lambda\boldsymbol{\Pi}+\mathbf{K})^{-1}\begin{pmatrix}f\\-f\end{pmatrix}=\frac{1}{2\lambda K}\begin{bmatrix}K+\frac{\lambda}{2} & K-\frac{\lambda}{2}\\ K-\frac{\lambda}{2} & K+\frac{\lambda}{2}\end{bmatrix}\begin{pmatrix}f\\-f\end{pmatrix}=\frac{1}{2\lambda K}\begin{pmatrix}\lambda f\\-\lambda f\end{pmatrix}=\frac{1}{K}\begin{pmatrix}\frac{f}{2}\\ \frac{-f}{2}\end{pmatrix}$$

Due to the singularity of $\boldsymbol{K}$, $\boldsymbol{x}$ can be expanded in a Laurent series,

$$\boldsymbol{x} = -\omega^{-2}\boldsymbol{x}_0+\omega^0\boldsymbol{x}_1+\omega^2\boldsymbol{x}_2 + \cdots+\omega^{2(p-1)}\boldsymbol{x}_p+\ldots \tag{A35}$$

Substituting equation (A35) into equation (A34) gives the identity

$$-\omega^{-2}\left(\boldsymbol{K}\boldsymbol{x}_0\right)+\omega^0\left(\boldsymbol{K}\boldsymbol{x}_1+\boldsymbol{M}\boldsymbol{x}_0-\boldsymbol{f}\right) +\omega^2\left(\boldsymbol{K}\boldsymbol{x}_2-\boldsymbol{M}\boldsymbol{x}_1\right)+\ldots=0, \tag{A36}$$

with the successive coefficients

$$\begin{aligned}\boldsymbol{T}_0 &= \boldsymbol{K}\boldsymbol{x}_0, \qquad \boldsymbol{T}_1=\boldsymbol{K}\boldsymbol{x}_1+\boldsymbol{M}\boldsymbol{x}_0-\boldsymbol{f},\\ \boldsymbol{T}_2 &= \boldsymbol{K}\boldsymbol{x}_2-\boldsymbol{M}\boldsymbol{x}_1, \qquad \ldots,\\ \boldsymbol{T}_{p-1} &= \boldsymbol{K}\boldsymbol{x}_p-\boldsymbol{M}\boldsymbol{x}_{p-1}, \qquad \ldots\end{aligned} \tag{A37}$$

must be set to zero to calculate the desired Laurent coefficients.

A3.2. Coefficient $\boldsymbol{x}_0$

Coefficient $\boldsymbol{x}_0$ is present in the first two relations in the cascade of relations (A37), namely:

$$\boldsymbol{K}\boldsymbol{x}_0=\boldsymbol{0}, \tag{A38}$$

$$\boldsymbol{K}\boldsymbol{x}_1+\boldsymbol{M}\boldsymbol{x}_0=\boldsymbol{f}. \tag{A39}$$

Unlike regular equations of ordinary linear algebra, where $\boldsymbol{A}\boldsymbol{x}=\boldsymbol{b}$ just means that $\boldsymbol{x}=\boldsymbol{A}^{-1}\boldsymbol{b}$, equations (A38) and (A39) provide a striking example of the tricky situations which are encountered with singular operators: because $\boldsymbol{K}$ is of rank $N-\sigma$, equation (A38) only gives $N-\sigma$ independent equations which are not sufficient to determine the N unknown components of $\boldsymbol{x}_0$. On the other hand, equation (A39), due to the regularity of $\boldsymbol{M}$, gives an expression of $\boldsymbol{x}_0$ in terms of $\boldsymbol{x}_1$, which is unfortunately unknown. The theorems developed in Appendix A2 are the only key to obtain the solution.

It comes out from equation (A38) and the definition of $\boldsymbol{S}$ that $\boldsymbol{x}_0$ is a rigid body motion of the form

$$\boldsymbol{x}_0=\boldsymbol{S}\boldsymbol{\gamma}. \tag{A40}$$

Writing equation (A39) in the form $\boldsymbol{K}\boldsymbol{x}_1=\boldsymbol{f}-\boldsymbol{M}\boldsymbol{x}_0$ shows, on the other hand, that $\boldsymbol{f}-\boldsymbol{M}\boldsymbol{x}_0$ is an element of range$\boldsymbol{K}$, which satisfies, by Lagrange lemma

$$\boldsymbol{S}^T\left(\boldsymbol{M}\boldsymbol{x}_0-\boldsymbol{f}\right)=0. \tag{A41}$$

It results then from equations (A40) and (A41) that the auxiliary unknown $\boldsymbol{\gamma}$ is solution to

$$\boldsymbol{S}^T\boldsymbol{M}\boldsymbol{S}\boldsymbol{\gamma}=\boldsymbol{S}^T\boldsymbol{f}. \tag{A42}$$

Table A2. Inertial expressions for the 2-mass 1D system of Figure A1.

1. Rigid body mass: $\mathbf{S}^{\mathrm{T}}\mathbf{M}\mathbf{S} = \begin{pmatrix}1 & 1\end{pmatrix}\begin{bmatrix}M_1 & 0\\ 0 & M_2\end{bmatrix}\begin{pmatrix}1\\1\end{pmatrix} = \begin{pmatrix}M_1 & M_2\end{pmatrix}\begin{pmatrix}1\\1\end{pmatrix} = M_1 + M_2$
2. Rigid body acceleration

$$(\mathbf{S}^{\mathrm{T}}\mathbf{M}\mathbf{S})^{-1}\mathbf{S}^{\mathrm{T}} = \frac{1}{M_1+M_2}\begin{pmatrix}1 & 1\end{pmatrix} \;;\; (\mathbf{S}^{\mathrm{T}}\mathbf{M}\mathbf{S})^{-1}\mathbf{S}^{\mathrm{T}}\begin{pmatrix}f_1\\f_2\end{pmatrix} = \frac{f_1+f_2}{M_1+M_2}$$

3. Distributed rigid body mass

$$\mathbf{S}(\mathbf{S}^{\mathrm{T}}\mathbf{M}\mathbf{S})^{-1}\mathbf{S}^{\mathrm{T}} = \frac{1}{M_1+M_2}\begin{pmatrix}1\\1\end{pmatrix}\begin{pmatrix}1 & 1\end{pmatrix} = \frac{1}{M_1+M_2}\begin{bmatrix}1 & 1\\ 1 & 1\end{bmatrix}$$

4. Distributed rigid body acceleration

$$\mathbf{S}(\mathbf{S}^{\mathrm{T}}\mathbf{M}\mathbf{S})^{-1}\mathbf{S}^{\mathrm{T}}\begin{pmatrix}f_1\\f_2\end{pmatrix} = \begin{pmatrix}\dfrac{f_1+f_2}{M_1+M_2}\\[2ex] \dfrac{f_1+f_2}{M_1+M_2}\end{pmatrix}$$

From this, there is no difficulty to express $\boldsymbol{x}_0$ as

$$\boldsymbol{x}_0 = \boldsymbol{S}\left(\boldsymbol{S}^T\boldsymbol{M}\boldsymbol{S}\right)^{-1}\boldsymbol{S}^T\boldsymbol{f}. \tag{A43}$$

It should be noticed that every term in the preceding equations can easily be interpreted in terms of elementary physics. In the most widespread engineering models, for example, stress-free motions are based on $\sigma = 6$ independent rigid- body motions, and

- $\boldsymbol{S}^T\boldsymbol{f} \in \mathsf{R}^6$ is the vector of resultants and moments corresponding to the given forces;
- $\boldsymbol{S}^T\boldsymbol{M}\boldsymbol{S}$ is the condensed 6x6 mass matrix that rules rigid body motions;
- $\boldsymbol{y} = (\boldsymbol{S}^T\boldsymbol{M}\boldsymbol{S})^{-1}\boldsymbol{S}^T\boldsymbol{f} \in \mathsf{R}^6$ gives the 6 intrinsic components of the rigid body acceleration;
- $\boldsymbol{S}\boldsymbol{y} = \boldsymbol{S}(\boldsymbol{S}^T\boldsymbol{M}\boldsymbol{S})^{-1}\boldsymbol{S}^T\boldsymbol{f}$ describes the complete rigid body acceleration field.

Table A2 details the precise expressions obtained for the system of one-dimensional masses of Appendix A2.

A3.3. Coefficient $\boldsymbol{x}_1$

Coefficient $\boldsymbol{x}_1$ only appears in relations $\boldsymbol{T}_1 = 0$ and $\boldsymbol{T}_2 = 0$ of cascade (A37), which gives

$$\boldsymbol{K}\boldsymbol{x}_1 + \boldsymbol{M}\boldsymbol{x}_0 = \boldsymbol{f}, \tag{A44}$$

$$\boldsymbol{K}\boldsymbol{x}_2 - \boldsymbol{M}\boldsymbol{x}_1 = \boldsymbol{0}. \tag{A45}$$

Substituting for $\boldsymbol{x}_0$ from equation (A43) into equation (A44) yields

$$\boldsymbol{K}\boldsymbol{x}_1 = \boldsymbol{f} - \boldsymbol{M}\boldsymbol{S}\left(\boldsymbol{S}^T\boldsymbol{M}\boldsymbol{S}\right)^{-1}\boldsymbol{S}^T\boldsymbol{f}. \tag{A46}$$

On the other hand, following the same argumentation developed in the above paragraph, equation (A45) shows that $\boldsymbol{M}\boldsymbol{x}_1$ is an element of range$\boldsymbol{K}$, which satisfies, by Lagrange lemma again,

$$\boldsymbol{S}^T\boldsymbol{M}\boldsymbol{x}_1 = 0. \tag{A47}$$

Equations (A46) and (A47) define a singular linear system of the type considered in the M-projector theorem of Appendix A2. It can be noted that the integrability condition

$$\boldsymbol{S}^T\left[\boldsymbol{f} - \boldsymbol{M}\boldsymbol{S}\left(\boldsymbol{S}^T\boldsymbol{M}\boldsymbol{S}\right)^{-1}\boldsymbol{S}^T\boldsymbol{f}\right] = 0 \tag{A48}$$

is satisfied, since the right member of equation (A46) results from the self-equilibrated combination of external loads with related inertia forces. The theorem thus gives

$$\boldsymbol{x}_1 = \left(1 - \boldsymbol{\Pi}_M\right)\left(\lambda\boldsymbol{\Pi} + \boldsymbol{K}\right)^{-1} \cdot \left[1 - \boldsymbol{M}\boldsymbol{S}\left(\boldsymbol{S}^T\boldsymbol{M}\boldsymbol{S}\right)^{-1}\boldsymbol{S}^T\right]\boldsymbol{f}. \tag{A49}$$

Using expression (A24) of the M-projector gives finally

$$\boldsymbol{x}_1 = \left(1 - \boldsymbol{\Pi}_M\right)\left(\lambda\boldsymbol{\Pi} + \boldsymbol{K}\right)^{-1}\left(1 - \boldsymbol{\Pi}_M^T\right)\boldsymbol{f}. \tag{A50}$$

Displacement $\boldsymbol{x}_1$ can be identified as the elastic displacement under external and inertial forces after adequate "filtration" of the rigid body modes. It is usually termed "inertia relief displacement". Precise expressions for the system of one-dimensional masses of Appendix A2 can be found in Table A3.

A3.4. Coefficients $\boldsymbol{x}_p$, $p \geq 2$

The periodical structure of relations (A37) for $p \geq 2$, means that the corresponding coefficients form a geometric progression. Writing conditions $\boldsymbol{T}_{p-1} = 0$ and $\boldsymbol{T}_p = 0$ for $p \geq 2$, leads to a sequence of singular systems

$$\boldsymbol{K}\boldsymbol{x}_p = \boldsymbol{M}\boldsymbol{x}_{p-1}, \tag{A51}$$

$$\boldsymbol{S}^T\boldsymbol{M}\boldsymbol{x}_p = \boldsymbol{0}. \tag{A52}$$

The integrability condition being easily proved at each stage by induction in the condition $\boldsymbol{S}^T\boldsymbol{M}\boldsymbol{x}_1 = \boldsymbol{0}$, the M-projector theorem gives one or the other equivalent expres-

Table A3. Inertia-relief expressions for the 2-mass 1D system of Figure A1.

1. M-projector onto $ker\,\mathbf{K}$:

$$\mathbf{\Pi}_M = \mathbf{S}\left(\mathbf{S}^{\mathrm{T}}\mathbf{M}\mathbf{S}\right)^{-1}\mathbf{S}^{\mathrm{T}}\mathbf{M} = \frac{1}{M_1+M_2}\begin{bmatrix}1 & 1\\ 1 & 1\end{bmatrix}\begin{bmatrix}M_1 & 0\\ 0 & M_2\end{bmatrix} = \begin{bmatrix}\frac{M_1}{M_1+M_2} & \frac{M_2}{M_1+M_2}\\ \frac{M_1}{M_1+M_2} & \frac{M_2}{M_1+M_2}\end{bmatrix}$$

2. Complementary M-projector ($\rightarrow$*M-orthogonalization with respect to rigid body motions*):

$$\mathbf{1}-\mathbf{\Pi}_M = \begin{bmatrix}1 & 0\\ 0 & 1\end{bmatrix} - \begin{bmatrix}\frac{M_1}{M_1+M_2} & \frac{M_2}{M_1+M_2}\\ \frac{M_1}{M_1+M_2} & \frac{M_2}{M_1+M_2}\end{bmatrix} = \begin{bmatrix}\frac{M_2}{M_1+M_2} & \frac{-M_2}{M_1+M_2}\\ \frac{-M_1}{M_1+M_2} & \frac{M_1}{M_1+M_2}\end{bmatrix}$$

3. Transposed complementary M-projector ($\rightarrow$*balancing of exterior forces with inertia forces*):

$$\mathbf{1}-\mathbf{\Pi}_M^{\mathrm{T}} = \begin{bmatrix}\frac{M_2}{M_1+M_2} & \frac{-M_1}{M_1+M_2}\\ \frac{-M_2}{M_1+M_2} & \frac{M_1}{M_1+M_2}\end{bmatrix} \quad ; \quad \left(\mathbf{1}-\mathbf{\Pi}_M^{\mathrm{T}}\right)\begin{pmatrix}f_1\\ f_2\end{pmatrix} = \begin{pmatrix}\frac{M_2 f_1 - M_1 f_2}{M_1+M_2}\\ \frac{-M_2 f_1 + M_1 f_2}{M_1+M_2}\end{pmatrix}$$

4. Distributor of inertia relief displacements under exterior and inertia forces:

$$\left(\mathbf{1}-\mathbf{\Pi}_M\right)\left(\lambda\mathbf{\Pi}+\mathbf{K}\right)^{-1}\left(\mathbf{1}-\mathbf{\Pi}_M^{\mathrm{T}}\right) = \cdots = \frac{1}{K}\begin{bmatrix}\left(\frac{M_2}{M_1+M_2}\right)^2 & \frac{-M_1M_2}{\left(M_1+M_2\right)^2}\\ \frac{-M_1M_2}{\left(M_1+M_2\right)^2} & \left(\frac{M_1}{M_1+M_2}\right)^2\end{bmatrix}$$

sions

$$\forall p \geq 2, \quad \boldsymbol{x}_p = \left(1-\mathbf{\Pi}_M\right)\left(\lambda\mathbf{\Pi}+\boldsymbol{K}\right)^{-1}\boldsymbol{M}\boldsymbol{x}_{p-1}, \tag{A53}$$

$$\forall p \geq 2, \quad \boldsymbol{x}_p = \Lambda^{p-1}\boldsymbol{x}_1, \tag{A54}$$

with $\Lambda = \left(1-\mathbf{\Pi}_M\right)\left(\lambda\mathbf{\Pi}+\boldsymbol{K}\right)^{-1}\boldsymbol{M}$.

A3.5. Laurent matrix coefficients

Laurent coefficients to be used in the expansion of global structural receptances can easily be identified to matrix coefficients appearing in equations (A43), (A50), (A53) and (A54) as

$$\boldsymbol{A}_0 = \boldsymbol{S}\left(\boldsymbol{S}^T\boldsymbol{M}\boldsymbol{S}\right)^{-1}\boldsymbol{S}^T, \tag{A55}$$

$$\boldsymbol{A}_1 = \left(1-\mathbf{\Pi}_M\right)\left(\lambda\mathbf{\Pi}+\boldsymbol{K}\right)^{-1}\left(1-\mathbf{\Pi}_M\right)^T, \tag{A56}$$

$$\forall p \geq 2, \quad \boldsymbol{A}_p = \left(1-\mathbf{\Pi}_M\right)\left(\lambda\mathbf{\Pi}+\boldsymbol{K}\right)^{-1}\boldsymbol{M}\boldsymbol{A}_{p-1}, \tag{A57}$$

$$\forall p \geq 2, \quad \boldsymbol{A}_p = \mathbf{\Lambda}^{p-1}\boldsymbol{A}_1, \tag{A58}$$

with $\mathbf{\Lambda} = \left(1-\mathbf{\Pi}_M\right)\left(\lambda\mathbf{\Pi}+\boldsymbol{K}\right)^{-1}\boldsymbol{M}$.

A4. Modal expressions of Taylor-Laurent coefficients and analysis of rank

Modal expressions are here used to analyze the singularity of full coefficients $\boldsymbol{A}_p$ and reduced coefficients $\boldsymbol{P}\boldsymbol{A}_p\boldsymbol{P}^T$ in Taylor-Laurent expansions. Although Taylor coefficients in fixed conditions of analysis are already known to be invertible matrices, their analysis is presented as an introduction to the modal approach.

A4.1. Taylor coefficients in fixed conditions of analysis

A4.1.1. Notations

It is known that it is always possible to find an M-orthonormal base of eigenmodes, $\boldsymbol{\psi}_m$, $m = 1, N$, associated to (circular) eigenfrequencies, ω_m, $\omega_1 \leq \omega_2 \leq \cdots \leq \omega_N$, such that

$$\left(\boldsymbol{K} - \boldsymbol{M}\omega_m^2\right)\boldsymbol{\psi}_m = 0. \tag{A59}$$

It is convenient to introduce an $N \times N$ diagonal matrix, $\mathbf{\Omega}$, and place eigenfrequencies, in ascending order, on the diagonal of $\mathbf{\Omega}$,

$$\mathbf{\Omega} = \mathrm{diag}\left(\{\omega_m\}_{m=1,\ldots,N}\right) = \begin{bmatrix}\omega_1 & 0 & \cdots & 0\\ 0 & \omega_2 & \cdots & 0\\ \vdots & \vdots & \ddots & \vdots\\ 0 & 0 & \cdots & \omega_N\end{bmatrix}. \tag{A60}$$

It is also useful to assemble eigenmodes along the N columns of an $N \times N$ modal matrix $\boldsymbol{\psi}$:

$$\boldsymbol{\psi} = \left[\psi_1\ \psi_2\ \ldots\ \psi_N\right]. \tag{A61}$$

Taylor coefficients. Mode-superposition expressions of responses of mechanical systems are the key to modal expansions of Taylor-Laurent coefficients. In fixed conditions of analysis both $\boldsymbol{K}$ and $\boldsymbol{M}$ are invertible matrices. In these circumstances, the overall receptance matrix is known to be given by an "ordinary modal summation"

$$\left(\boldsymbol{K}-\omega^2\boldsymbol{M}\right)^{-1} = \boldsymbol{\psi}\mathrm{diag}\left(\left\{\frac{l}{\omega_m^2-\omega^2}\right\}_{m=1,\dots,N}\right)\boldsymbol{\psi}^T. \tag{A62}$$

It is also possible to use an equivalent modal formula [19]

$$\left(\boldsymbol{K}-\omega^2\boldsymbol{M}\right)^{-1} = \boldsymbol{K}^{-1}+\boldsymbol{\psi}\mathrm{diag}\left(\left\{\frac{\omega^2}{\omega_m^2}\frac{l}{\omega_m^2-\omega^2}\right\}_{m=1,\dots,N}\right)\boldsymbol{\psi}^T \tag{A63}$$

that can either be termed an "accelerated modal summation", if one considers the ω^2/ω_m^2 factor in high order modal components, or a "modal summation with static correction", if one considers the static term, $\boldsymbol{K}^{-1}$.

Proceeding to geometric expansions of the form $(1-x)^{-1} = 1+x+x^2+\cdots+x^m+\dots$ of the diagonal terms of modal decompositions, transform the latter into Taylor expansions at origin. Starting either with (A62) or (A63) leads to identical expressions $\boldsymbol{A}_p = \boldsymbol{\psi}\boldsymbol{\Omega}^{-2p}\boldsymbol{\psi}^T$ for every $p \geq 2$.

Depending on whether ordinary formulae (A62) or accelerated formulae (A63) are used, the static $\boldsymbol{A}_1$-term can either be given as $\boldsymbol{A}_1 = \boldsymbol{\psi}\boldsymbol{\Omega}^{-2}\boldsymbol{\psi}^T$ or $\boldsymbol{A}_1 = \boldsymbol{K}^{-1}$. This clearly designates the modal expression of this term as the weak link of the chain in possible applications of the reduction technique in an experimental context. Considering however that in the present theoretical study, $\boldsymbol{\psi}$ and $\boldsymbol{\Omega}$ are complete $N \times N$ matrices gathering all modal data, it is possible to express overall Taylor coefficients by

$$\boldsymbol{A}_1 = \boldsymbol{\psi}\boldsymbol{\Omega}^{-2p}\boldsymbol{\psi}^T \tag{A64}$$

and, after reduction through a P-matrix , by

$$\boldsymbol{a}_p = \left(\boldsymbol{P}\boldsymbol{\psi}\right)\boldsymbol{\Omega}^{-2p}\left(\boldsymbol{P}\boldsymbol{\psi}\right)^T. \tag{A65}$$

A4.1.2. Analysis of rank

The main interest of modal expressions, like those appearing in equations (A64) and (A65), lies in the fact that applying the following lemma, immediately reveals the kernels, ranges and ranks of the considered coefficients.

Symmetric decomposition lemma. *For any symmetric $p \times p$ matrix of the form $\boldsymbol{a}\boldsymbol{Q}\boldsymbol{a}^T$, where $\boldsymbol{a}$ is a $p \times q$ rectangular matrix, and $\boldsymbol{Q}$ is a symmetric strictly positive $q \times q$ matrix*

$$\ker\left(\boldsymbol{a}\boldsymbol{Q}\boldsymbol{a}^T\right) = \ker\boldsymbol{a}^T. \tag{A66}$$

The application of Lagrange lemma gives

$$\mathrm{range}\left(\boldsymbol{a}\boldsymbol{Q}\boldsymbol{a}^T\right) = \mathrm{range}\boldsymbol{a}, \tag{A67}$$

$$\mathrm{rank}\left(\boldsymbol{a}\boldsymbol{Q}\boldsymbol{a}^T\right) = \mathrm{rank}\boldsymbol{a}. \tag{A68}$$

Proof. It is clear that $\ker\boldsymbol{a}^T \subset \ker(\boldsymbol{a}\boldsymbol{Q}\boldsymbol{a}^T)$ since $\boldsymbol{a}^T\boldsymbol{x} = 0$ implies that $\boldsymbol{a}\boldsymbol{Q}\boldsymbol{a}^T\boldsymbol{x} = 0$. The reverse inclusion $\ker(\boldsymbol{a}\boldsymbol{Q}\boldsymbol{a}^T) \subset \ker\boldsymbol{a}^T$ comes from the fact that any vector $\boldsymbol{x}$ such that $\boldsymbol{a}\boldsymbol{Q}\boldsymbol{a}^T\boldsymbol{x} = 0$ satisfies $\boldsymbol{x}^T\boldsymbol{a}\boldsymbol{Q}\boldsymbol{a}^T\boldsymbol{x} = (\boldsymbol{a}^T\boldsymbol{x})^T\boldsymbol{Q}\boldsymbol{a}^T\boldsymbol{x} = 0$, and thus $\boldsymbol{a}^T\boldsymbol{x} = 0$ since $\boldsymbol{Q}$ is strictly positive.

Because $\boldsymbol{\Omega}^{-2p} > 0$ and $\boldsymbol{\psi}$ is a regular $N \times N$ matrix, applying the lemma to equation (A64) leads to the conclusion that $\boldsymbol{A}_p$ are invertible matrices satisfying

$$\ker\boldsymbol{A}_p = \ker\boldsymbol{\psi}^T = \{\boldsymbol{0}\}. \tag{A69}$$

Applying the lemma to reduced Taylor coefficients given by equation (A65), results in the conclusion that $\ker\boldsymbol{a}_p = \ker(\boldsymbol{P}\boldsymbol{\psi})^T$ consists of vectors $\boldsymbol{x} \in \mathbb{R}^n$ that satisfy $\boldsymbol{\psi}^T\boldsymbol{P}^T\boldsymbol{x} = 0$, or, by the regularity of $\boldsymbol{\psi}$, $\boldsymbol{P}^T\boldsymbol{x} = 0$. Provided $\boldsymbol{P}$ is a matrix of maximum rank n, corresponding to n independent observations, the n rows of $\boldsymbol{P}^T$ are linearly independent, and the latter condition necessarily implies that $\boldsymbol{x} = 0$. Reduced Taylor coefficients can thus be recognized as invertible matrices satisfying

$$\ker\boldsymbol{a}_p = \{\boldsymbol{0}\}. \tag{A70}$$

Relations (A69) and (A70) confirm the property of regularity of Taylor coefficients, that have already been observed in section 2.

A4.2. Laurent coefficients in free-floating conditions of analysis

A4.2.1. Notations

In free-floating conditions, the stiffness matrix, $\boldsymbol{K}$, has $\sigma > 0$ eigenvectors associated with zero eigenvalues, which form a system of $\sigma > 0$ eigenmodes at zero frequency. Splitting up the $N \times N$ modal matrix in a $\sigma \times N$ modal matrix related to modes at zero frequency, and a $(N-\sigma) \times N$ modal matrix corresponding to modes at strictly positive frequencies leads to

$$\boldsymbol{\psi}_0 = \left[\psi_1\ \psi_2\ \dots\ \psi_\sigma\right], \tag{A71}$$

$$\boldsymbol{\psi}^+ = \left[\psi_{\sigma+1}\ \psi_{\sigma+2}\ \dots\ \psi_N\right]. \tag{A72}$$

Finally, the strictly positive eigenfrequencies can be extracted from the diagonal matrix $\boldsymbol{\Omega}$ to be assembled in a $(N-\sigma) \times (N-\sigma)$ block

$$\boldsymbol{\Omega}^+ = \mathrm{diag}\left(\{\omega_m\}_{m=\sigma+1,\dots,N}\right) = \begin{bmatrix} \omega_{\sigma+1} & 0 & \cdots & 0 \\ 0 & \omega_{\sigma+2} & \cdots & 0 \\ \vdots & \vdots & \ddots & \vdots \\ 0 & 0 & \cdots & \omega_N \end{bmatrix}. \tag{A73}$$

A4.2.2. Modal expression of Laurent coefficients

As in the fixed conditions of analysis, the modal expressions of Laurent coefficients can be obtained from mode-superposition formulae. With the preceding notations, ordinary modal decompositions can be written as

$$\left(\boldsymbol{K}-\omega^2\boldsymbol{M}\right)^{-1} = -\frac{\boldsymbol{\psi}_0\boldsymbol{\psi}_0^T}{\omega^2}+\boldsymbol{\psi}^+\mathrm{diag}\left(\left\{\frac{1}{\omega_m^2-\omega^2}\right\}_{m=\sigma+1,\dots,N}\right)\boldsymbol{\psi}^{+T}. \tag{A74}$$

while "accelerated" decompositions, as shown in [19], are given by

$$\big(\boldsymbol{K}-\omega^2\boldsymbol{M}\big)^{-1} = \tag{A75}$$
$$-\frac{\boldsymbol{\psi}_0\boldsymbol{\psi}_0^T}{\omega^2}+\big(1-\boldsymbol{\Pi}_M\big)\big(\lambda\boldsymbol{\Pi}+\boldsymbol{K}\big)^{-l}\big(1-\boldsymbol{\Pi}_M^T\big)+\ldots$$
$$+\boldsymbol{\psi}^{+}\mathrm{diag}\left(\left\{\frac{\omega^2}{\omega_m^2}\frac{1}{\omega_m^2-\omega^2}\right\}_{m=\sigma+1,\ldots,N}\right)(\boldsymbol{\psi}^{+})^T.$$

Geometric expansions give, as before, the following expressions of global Laurent coefficients

$$\boldsymbol{A}_0 = \boldsymbol{\psi}_0\boldsymbol{\psi}_0^T, \tag{A76}$$
$$\boldsymbol{A}_p = \boldsymbol{\psi}^{+}\big(\boldsymbol{\Omega}\big)^{-2p}\boldsymbol{\psi}^{+T}, \quad p\geq 1. \tag{A77}$$

Accelerated formulae give the same results except for the $\boldsymbol{A}_1$-term. The theoretical analysis of the singularity of overall Laurent coefficients can be based on formulae (A76) and (A77). Similarly, the analysis of the reduced coefficients can be based on

$$\hat{\boldsymbol{a}}_0 = \big(\boldsymbol{P}\boldsymbol{\psi}_0\big)\big(\boldsymbol{P}\boldsymbol{\psi}_0\big)^T \tag{A78}$$
$$\hat{\boldsymbol{a}}_p = \big(\boldsymbol{P}\boldsymbol{\psi}^{+}\big)\big(\boldsymbol{\Omega}^{+}\big)^{-2p}\big(\boldsymbol{P}\boldsymbol{\psi}^{+}\big)^T, \quad p\geq 1. \tag{A79}$$

A4.2.3. Analysis of rank

The application of the symmetric decomposition lemma of §1.3 to the expressions (A76) and (A77) of Laurent coefficients leads to

$$\mathrm{ker}\boldsymbol{A}_0 = \mathrm{ker}\boldsymbol{\psi}_0^T, \qquad \mathrm{range}\boldsymbol{A}_0 = \mathrm{range}\boldsymbol{\psi}_0,$$
$$\mathrm{rank}\boldsymbol{A}_0 = N, \tag{A80}$$

for each $p\geq 1$:

$$\mathrm{ker}\boldsymbol{A}_p = \mathrm{ker}\boldsymbol{\psi}^{+T}, \qquad \mathrm{range}\boldsymbol{A}_p = \mathrm{range}\boldsymbol{\psi}^{+},$$
$$\mathrm{rank}\boldsymbol{A}_p = N-\sigma. \tag{A81}$$

It results from the general property of M-orthogonality of the eigen-subspaces that $\boldsymbol{\psi}^{+} = (\boldsymbol{M}\boldsymbol{\psi}_0)^{\perp}$. Moreover, the identity of stress- free motions and inertial modes means that $((\boldsymbol{\psi}_0)) = ((\boldsymbol{S}))$, where $\boldsymbol{S}$ stands for the spanning matrix of $\ker\boldsymbol{K}$ which is used throughout the text. Equations (A80) and (A81) can therefore be written as

$$\mathrm{ker}\boldsymbol{A}_0 = \big((\boldsymbol{S})\big)^{\perp}, \qquad \mathrm{range}\boldsymbol{A}_0 = \big((\boldsymbol{S})\big),$$
$$\mathrm{rank}\boldsymbol{A}_0 = \sigma, \tag{A82}$$

for each $p\geq 1$:

$$\mathrm{ker}\boldsymbol{A}_p = \big((\boldsymbol{M}\boldsymbol{S})\big), \qquad \mathrm{range}\boldsymbol{A}_p = \big((\boldsymbol{M}\boldsymbol{S})\big)^{\perp},$$
$$\mathrm{rank}\boldsymbol{A}_p = N-\sigma. \tag{A83}$$

Similarly, reduced coefficients of equations (A78) and (A79) can easily be seen to verify

$$\mathrm{ker}\hat{\boldsymbol{a}}_0 = \big(\boldsymbol{P}\boldsymbol{\psi}_0\big)^T, \quad \mathrm{range}\hat{\boldsymbol{a}}_0 = \mathrm{range}\big(\boldsymbol{P}\boldsymbol{\psi}_0\big), \tag{A84}$$

for each $p\geq 1$:

$$\mathrm{ker}\hat{\boldsymbol{a}}_p = \big(\boldsymbol{P}\boldsymbol{\psi}^{+}\big)^T, \quad \mathrm{range}\hat{\boldsymbol{a}}_p = \mathrm{range}\big(\boldsymbol{P}\boldsymbol{\psi}^{+}\big). \tag{A85}$$

Equations (A84) can be rewritten as

$$\mathrm{ker}\hat{\boldsymbol{a}}_0 = \big((\boldsymbol{P}\boldsymbol{S})\big)^{\perp}, \quad \mathrm{range}\hat{\boldsymbol{a}}_0 = \big((\boldsymbol{P}\boldsymbol{S})\big),$$
$$\mathrm{rank}\hat{\boldsymbol{a}}_0 = \hat{\sigma} = \dim\big((\boldsymbol{P}\boldsymbol{S})\big)\leq\sigma. \tag{A86}$$

There is few to comment about, except that ((PS)) correspond to what is observed in the set of stress-free motions through the P-matrix, and it is of dimension σ less than or equal to σ.

The fact that most of the time, formulae (A85) refer to invertible matrices is far from being obvious. This point is of a capital importance in the Censoring-Covering algorithm and thus deserves a quite special attention.

First consider a strict reduction with a $n\times N$ localization matrix of the form $\boldsymbol{P} = [\boldsymbol{1}_{aa}\ \boldsymbol{0}_{ad}]$, where a and d denote the retained and deleted coordinates. Matrix $\boldsymbol{P}\boldsymbol{\psi}^{+}$ in this circumstance is just the $n\times N-\sigma$ block, $\boldsymbol{\psi}_a^{+}$, inside the global $n\times N-\sigma$ modal matrix $\boldsymbol{\psi}^{+}$, which corresponds to the retained coordinates. Matrix $\boldsymbol{\psi}^{+}$ is of rank $N-\sigma$ because its columns are independent eigenmodes. By Lagrange lemma, the N rows of $\boldsymbol{\psi}^{+}$ form a system of vectors of rank $N-\sigma$, in which non-trivial zero combinations cannot be obtained with less than $N-\sigma$ terms. Consequently, the n rows in $\boldsymbol{\psi}_a^{+}$ are linearly independent provided $n\leq N-\sigma$, i.e. in all practical circumstances. Coefficient $\hat{\boldsymbol{a}}_p$ are therefore of rank n, and conditions (A85) can indeed be rewritten as

for each $p\geq 1$:

$$\mathrm{ker}\hat{\boldsymbol{a}}_p = \{0\}, \quad \mathrm{range}\hat{\boldsymbol{a}}_p = \mathbf{R}^n, \quad \mathrm{rank}\hat{\boldsymbol{a}}_p = n. \tag{A87}$$

Contraction can be generally thought as bringing the invertibility, and it is clear that most reductions in generalized coordinates will lead to similar conditions. A notable exception however exists, which remains to be fully understood and integrated into a theory of generalized reductions. This exception concerns generalized coordinates of the form $\boldsymbol{M}\boldsymbol{S}$, such as they appear in equations (A83), corresponding to the images of the stress-free motions through the mass matrix. The point is that augmenting, for example, a strict P-matrix by a $\sigma\times N$ block, $\boldsymbol{S}^T\boldsymbol{M}$, corresponding to such coordinates, gives the relation

$$\mathrm{range}\hat{\boldsymbol{a}}_p = \mathrm{range}\left(\begin{bmatrix}\boldsymbol{1}_{aa} & 0\\ \boldsymbol{S}^T\boldsymbol{M}\end{bmatrix}\boldsymbol{\psi}^{+}\right)$$
$$= \mathrm{range}\left(\begin{bmatrix}\boldsymbol{\psi}_a^{+}\\ 0_{\sigma\times N}\end{bmatrix}\right), \tag{A88}$$

which leads to the observation that reduced coefficients $\hat{\boldsymbol{a}}_p$ are singular matrices as for the coefficients $\boldsymbol{A}_p$ in the free-floating global system.

References

[1] R. J. Guyan: Reduction of stiffness and mass matrices. AIAA J. **3** (1969) 380.

[2] J. R. R. Craig, A. J. Kurdila: Fundamentals of structural dynamics, 2nd ed. John Wiley & Sons, Inc., Hoboken, New Jersey, 2006.

[3] D. de Klerk, D. J. Rixen, S. N. Voormeeren: General framework for dynamic substructuring: History, review, and classification of techniques. AIAA J. **46** (2008).

[4] J. R. R. Craig, M. C. Bampton: Coupling of substructures for dynamic analyses. AIAA J. **6** (1968) 1313–1319.

[5] J. R. R. Craig, M. C. Bampton: Coupling of substructures for dynamic analyses. AIAA J. **6** (1968) 1313–1319.

[6] R. H. MacNeal: A hybrid method of component mode synthesis. Computers and Structures **1** (1971) 581–601.

[7] G. M. L. Gladwell: Branch mode analysis of vibrating systems. Journal of Sound and Vibration **1** (1964) 41–59.

[8] E. Balmès: Optimal Ritz vectors for component mode synthesis using the singular value decomposition. AIAA Journal **34** (1996).

[9] E. Balmès: Use of generalized interface degrees of freedom in component mode synthesis. IMAC 1996 (1996) 204–210.

[10] N. Roy: Vibro-acoustic responses to a diffuse acoustic field. MSC Nastran User Conference, Toulouse, France, 2010.

[11] M. Ainsworth, J. T. Oden: A posteriori error estimation in finite element analysis. John Wiley & Sons, New York, 2000.

[12] F. Ihlenburg: Finite element analysis of acoustic scattering. Springer Verlag, New York, 1998.

[13] J.-M. Lagache, S. Assaf, O. Sauvage: Modal synthesis using accelerated modal summations. Proceedings of ISMA 2008, Katholieke Universiteit Leuven, 2008.

[14] J.-M. Lagache, S. Assaf: Explicit Mac Neal model reduction using accelerated modal formulae. Proceedings of ICSV 16, Silesian University of Technology, Krakow, 2009.

[15] S. Assaf, J.-M. Lagache: Elimination of internal structural variables through explicit Mac-Neal modal reduction. Euronoise 2009, Edinburgh, 2009.

[16] J.-M. Lagache, S. Assaf: An explicit algebraic reduction technique, involving physical, generalized or modal coordinates. ISMA 2010 Noise and Vibration Engineering conference, Leuven, 2010.

[17] J.-M. Lagache, S. Assaf: Algebraic reduction of finite-element acoustic models. 17th symposium on Vibrations, Shocks and Noise, Lyon, 2010.

[18] G. Strang: Introduction to applied mathematics. Wellesley-Cambridge Press, Wellesley, Massachussets, 1986.

[19] J.-M. Lagache, S. Assaf, C. Schulte: Finite element synthesis of structural or acoustic receptances in view of practical design applications. Journal of Sound and Vibration **310** (2008) 313–351.

[20] S. Assaf, M. Guerich: Numerical prediction of noise transmission loss through viscoelastically damped sandwich plates. Journal of Sandwich Structures and Materials **10** (2008) 359–384.

[21] S. Assaf: Finite element formulation of vibrations of sandwich beams and plates: steel-viscoelastic materials (in French). Ph.D. Thesis, Université de Technologie de Compiègne, France, 1991.

[22] C. D. Johnson, D. A. Kienholz, L. C. Rogers: Finite element prediction of damping in beams with constrained viscoelastic layers. AIAA Journal **20** (1982) 71–81.

[23] R. Rikards, A. Chate, E. Barkanov: Finite element analysis of damping the vibrations of laminated composites. Computers and Structures **47** (1993) 1005–1015.

[24] O. Foin, J. Nicolas, N. Atalla: An efficient tool for predicting the structural acoustic and vibration response of sandwich plates in light or heavy fluid. Applied Acoustics **57** (1999) 213–242.

[25] C. Lee, K. Kondo: Noise transmission loss of sandwich plates with viscoelastic core. AIAA 1999, Proceedings of Structural Dynamics and Materials Conference and Exhibit, 40th, St. Louis, MO, 1999, 2137–2147.

[26] V. Guillemin, A. Pollack: Differential topology. Prentice-Hall, Inc., Englewood Cliffs, New Jersey, 1974.

[27] S. Botello, E. O. nate, J. M. Canet: A layer-wise triangle for analysis of laminated composite plates and shells. Computers and Structures **70** (1999) 635–646.

[28] E. Carrera: Theories and finite elements for multilayered plates and shells: A unified compact formulation with numerical assessment and benchmarking. Arch. Comput. Meth. Eng. **10** (2003) 215–296.

[29] A. D. Nashif, D. I. G. Jones, J. P. Henderson: Vibration damping. John Wiley & Sons, New York, 1985.

[30] S. H. Zhang, H. L. Chen: A study on the damping characteristics of laminated composites with integral viscoelastic layers. Composites Structures **74** (2006) 63–69.

[31] M. D. Rao, R. Echempati, S. Nadella: Dynamic analysis and damping of composite structures embedded with viscoelastic layers. Composites Part B **28** (1997) 547–554.

[32] J. Ben Mariem, M. A. Hamdi: A new boundary finite element method for fluid-structure interaction problems. International Journal for Numerical Methods in Engineering **24** (1987) 1251–1267.